Available online at www.sciencedirect.com
ScienceDirect
International Journal of Solids and Structures 45 (2008) 794–820
INTERNATIONAL JOURNAL OF SOLIDS AND STRUCTURES
www.elsevier.com/locate/ijsolstr

Elastic layers bonded to flexible reinforcements

Seval Pinarbasi [a,*], Yalcin Mengi [b]

[a] Department of Civil Engineering, Middle East Technical University, 06531 Ankara, Turkey
[b] Department of Engineering Sciences, Middle East Technical University, 06531 Ankara, Turkey

Received 14 June 2007; received in revised form 12 August 2007
Available online 14 September 2007

Abstract

Elastic layers bonded to reinforcing sheets are widely used in many engineering applications. While in most of the earlier applications, these layers are reinforced using steel plates, recent studies propose to replace ''rigid'' steel reinforcement with ''flexible'' fiber reinforcement to reduce both the cost and weight of the units/systems. In this study, a new formulation is presented for the analysis of elastic layers bonded to flexible reinforcements under (i) uniform compression, (ii) pure bending and (iii) pure warping. This new formulation has some distinct advantages over the others in literature. Since the displacement boundary conditions are included in the formulation, there is no need to start the formulation with some assumptions (other than those imposed by the order of the theory) on stress and/or displacement distributions in the layer or with some limitations on geometrical and material properties. Thus, the solutions derived from this formulation are valid not only for ''thin'' layers of strictly or nearly incompressible materials but also for ''thick'' layers and/or compressible materials. After presenting the formulation in its most general form, with regard to the order of the theory and shape of the layer, its applications are demonstrated by solving the governing equations for bonded layers of infinite-strip shape using zeroth and/or first order theory. For each deformation mode, closed-form expressions are obtained for displacement/stress distributions and effective layer modulus. The effects of three key parameters: (i) shape factor of the layer, (ii) Poisson's ratio of the layer material and (iii) extensibility of the reinforcing sheets, on the layer behavior are also studied.

Keywords: Bonded elastic layer; Flexible reinforcement; Compression; Bending; Warping; Shape factor; Poisson's ratio; Galerkin method; Rubber; Elastomeric bearing; Seismic isolation

1. Introduction

Elastic layers bonded to reinforcing sheets have long been used as suspension and support systems, compression and shear mountings, and as sealing components. It is now very well known that the compression/bending stiffness of a bonded elastic layer may be several orders of magnitude greater than that of the corresponding unbonded layer (Gent and Lindley, 1959). Despite their significant effects on the compressive

* Corresponding author. Tel.: +90 312 210 54 64; fax: +90 312 210 11 93.
E-mail address: sevalp@metu.edu.tr (S. Pinarbasi).

0020-7683/$ - see front matter © 2007 Elsevier Ltd. All rights reserved.
doi:10.1016/j.ijsolstr.2007.08.029

or bending behavior, the reinforcing sheets do *not* influence the shear behavior of a bonded elastic layer considerably. This is an important property considering that the resistance of a soft elastic layer to compression and bending can be increased without compromising from its flexibility in shear.

Composed of several elastomer layers sandwiched between and bonded to reinforcing sheets, elastomeric bearings have been developed using this favorable mechanical property of bonded elastic layers. In the earlier applications, elastomeric bearings were primarily used as bridge bearings, helicopter rotor bearings, wharf fenders and elastic foundations to machinery and motors. Recently, their applications have been extended to seismic isolation, which is a new earthquake resistant design concept in which flexible elements are inserted at the base of the structure to reduce the transmission of seismic force from soil to the structure. While most of the elastomeric bearings used in seismic isolation are reinforced with steel plates, in a recent study, Kelly (1999) proposed to replace steel reinforcement with fiber reinforcement to produce cost-effective light-weight isolators to be used in developing countries. Since with recent technology, it is conceivable to produce fiber materials with elastic stiffness comparable to that of steel, "it is possible to produce a fiber reinforced bearing that matches the behavior of steel reinforced bearing (Tsai and Kelly, 2002)". Although the idea of replacing the steel reinforcement with some kinds of fiber reinforcement in seismic isolation bearings is new, the viability of the concept has already been investigated through several experimental studies (e.g., Moon et al., 2002; Kelly, 2002; Kelly and Takhirov, 2001, 2002).

Similar to the steel-reinforced case, most of the analytical studies on fiber-reinforced bearings are conducted on an individual elastomer layer bonded to flexible reinforcements. There is an important difference between the analysis of these two cases: while in the analysis of a steel-reinforced elastic layer, the reinforcement is assumed to be "rigid both in extension and flexure", in the analysis of a fiber-reinforced elastic layer, it is assumed to be "flexible in extension but completely without flexure rigidity" (Kelly, 2002).

As reviewed in Pinarbasi et al. (2006) in detail, in the last century, many researchers (e.g., Lindley, 1979; Gent, 1994; Horton et al., 2002) have studied the behavior of rigidly-bonded elastic layers. Most of these studies have been conducted to determine their compression stiffness. According to Kelly (1997), "the first analysis of the compression stiffness was done using an energy approach by Rocard" in 1937 "and further developments were made by Gent and Lindley (1959) and Gent and Meinecke (1970)". These earliest studies, conducted using small deformation theory, put forward three basic assumptions:

(i) horizontal plane sections remain plane after deformation,
(ii) initially vertical lateral surfaces take a parabolic shape in the deformed configuration (parabolic bulging assumption),
(iii) state of stress at any point in the material is dominated by the hydrostatic pressure ("pressure" assumption).

It is to be noted that these fundamental assumptions lead to the same differential equation in terms of the "pressure" term, which is commonly called as "pressure equation", even when different formulations are used. For this reason, it is common to name all of the formulations developed based on these three fundamental assumptions the "pressure method".

The effect of reinforcement extensibility on behavior of bonded elastic layers has been studied in a series of works by disregarding the flexural rigidity of the reinforcing sheets. Kelly (1999) analyzed the compressive and bending behavior of an infinite-strip-shaped rubber layer bonded to flexible reinforcements by using the pressure method and assuming strict incompressibility. His approach was later applied to rectangular and circular shapes by Tsai and Kelly (2001). The incompressibility assumption was released by Kelly (2002), who derived a closed-form expression for compression modulus of infinite-strip-shaped layers for compressible materials. The studies of Tsai (2004, 2006) are different from the study of Kelly (2002) in that Tsai further removed the stress assumption of the pressure method in his formulation. The works by Kelly (1994) and Tsai and Kelly (2005b) are more general than the others in the sense that they included in their formulation the "warping" (distortional deformations) of the reinforcing sheets (Fig. 1d), besides the compressional (Fig. 1b) and bending (Fig. 1c) deformations of the layer (Fig. 1a). As emphasized by Tsai and Kelly (2005a), "the terminology of warping used here is *not* associated with torsion; it just specifies the distortion of the cross-section created by moment and shear".

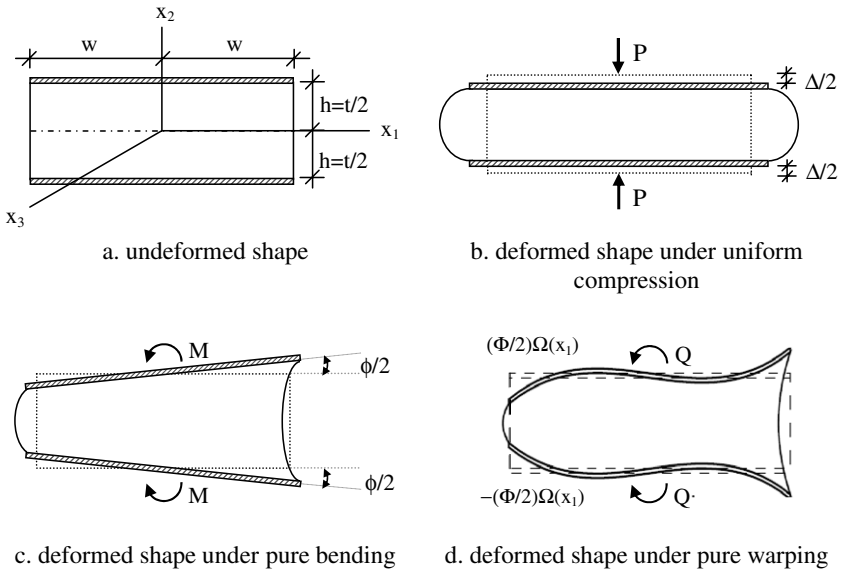

a. undeformed shape

b. deformed shape under uniform compression

c. deformed shape under pure bending

d. deformed shape under pure warping

Fig. 1. Undeformed and deformed configurations for an elastic layer bonded to flexible reinforcements under uniform compression, pure bending and pure warping (taken from Tsai and Kelly (2005b)).

From the above review, it is clear that there are only a few studies in literature on elastic layers bonded to extensible reinforcements, most of which have focused on the derivation of closed-form expressions for the effective layer moduli. On the other hand, as emphasized by Gent et al. (1974), the knowledge on detailed displacement/stress distributions and locations/magnitudes of critical stresses in the layer is also essential for a rational design.

Recently, a new analytical approach was formulated by Pinarbasi et al. (2006) for linear analysis of rigidly-bonded elastic layers under their basic deformation modes; (i) uniform compression, (ii) pure bending and (iii) apparent shear. Developed using an approximate theory due to Mengi (1980), this new formulation has some distinct advantages over the others in literature; it permits (i) eliminating the need for the assumptions (other than those imposed by the order of the theory) on displacement/stress distributions in the layer, (ii) including the material compressibility, (iii) being applicable to layers of any symmetrical shape, (iv) performing the analysis in a systematic manner and (v) being open to improvement.

In this study, the formulation proposed by Pinarbasi et al. (2006) is extended to elastic layers bonded to extensible reinforcements. Unlike the rigid reinforcement case, the warping (distortion) of the reinforcements has to be considered in the flexible reinforcement case when the layer undergoes bending or shear deformations. In this paper (for the flexible case), only the compression and bending modes are considered; the study of the shear mode is left to a future study. It is obvious that, for the flexible reinforcement case, the compression mode (Fig. 1b) does not involve warping while the bending mode may be considered to be composed of two simpler modes: pure bending (Fig. 1c) and pure warping (Fig. 1d).

In the paper, for each deformation mode, keeping the order of the theory and shape of the layer arbitrary, the relevant equations are first presented in general forms, in view of the displacement boundary conditions at the top and bottom faces of the layer, and the determination of displacement/stress distributions and relevant effective modulus is discussed. The governing equations derived for this case are, then, solved for infinite-strip-shaped layers using zeroth and/or first order theories to obtain analytical solutions for each deformation mode. Closed form expressions derived for displacement/stress distributions and three effective moduli; compression, bending and warping moduli, are later used to investigate the effects of three main parameters: (i) aspect ratio of the layer, (ii) compressibility of the layer material and (iii) extensibility of the reinforcing sheets, on the layer behavior.

2. Review of the approximate theory used in the study

The new analytical approach used in this study for the analysis of elastic layers bonded to flexible reinforcing sheets is developed from an approximate theory due to Mengi (1980). In this section, this approximate theory is reviewed very briefly to introduce the notation used in the formulation; for details, Pinarbasi et al. (2006) and Mengi (1980) may be referred to.

Formulated originally to analyze the dynamic behavior of thermoelastic plates by using a modified version of the Galerkin Method, this approximate theory assumes that the material is isotropic and linearly elastic and that the layer has a uniform thickness of $2h$. The layer is referred to a Cartesian coordinate system (x_1 x_2 x_3), where the x_1x_3 plane coincides the mid-plane of the layer as shown in Fig. 1a. The theory contains two types of field variables: (i) "generalized variables" representing the *weighted* averages of displacements (u_i, $i = 1$–3) and stresses (τ_{ij}, $i,j = 1$–3) over the thickness of the layer, which are denoted respectively by u_i^n and τ_{ij}^n where $n = 0$–m for the mth order theory, and (ii) "face variables" denoting the components of displacements and tractions on the lateral faces of the layer, which are, respectively: $u_i^{\pm} = u_i|_{x_2=\pm h}$ and $\tau_{2i}^{\pm} = \tau_{2i}|_{x_2=\pm h}$. The main difference of the theory due to Mengi (1980) over the others in literature is that the inclusion of face variables as field variables in this theory eliminates any inconsistency which may exist between displacement distributions assumed over the thickness of the layer and boundary conditions on its flat faces.

In the development of the theory, a set of distribution functions $\phi_n(\bar{x}_2)$ ($n = 0,1,2,\ldots$; $\bar{x}_2 = x_2/h$) is chosen. For mth order theory, the elements ϕ_n (n =0–($m + 2$)) are retained in the set. Keeping the last two elements in the set is essential for establishing the constitutive equations for the face variables. The theory is basically composed of two sets of equations. The "weighted averages of elasticity equations" are obtained by applying the operator $L^n = \frac{1}{2h}\int_{-h}^{+h}(.)\phi_n \mathrm{d}x_2$, where ϕ_n ($n = 0$–m) are used as weighting functions, to the equilibrium and constitutive equations of linear elasticity. The "constitutive equations for face variables" are obtained through the expansion of displacements in terms of the distribution functions as $u_i = \sum_{k=0}^{m+2} a_k^i \phi_k$ and using it in the exact constitutive equations of tractions on flat faces of the layer, where a_k^i are some coefficients which are the functions of x_1 and x_3. These coefficients, upon the choice of distribution functions, may be related to the field variables of the approximate theory.

For an elastic layer bonded to reinforcing plates at its top and bottom faces, the approximate theory has the following governing equations:

- weighted form of equilibrium equations ($n = 0$–m):

$$\partial_1 \tau_{1i}^n + \partial_3 \tau_{3i}^n + (R_i^n - \bar{\tau}_{2i}^n) = 0 \quad (i = 1\text{–}3) \tag{1}$$

where

$$R_i^n = \frac{\hat{R}_i^n \phi_n(1)}{2h} \quad \text{where } \hat{R}_i^n = \begin{cases} R_i^- = \tau_{2i}^+ - \tau_{2i}^- & \text{for even } n \\ R_i^+ = \tau_{2i}^+ + \tau_{2i}^- & \text{for odd } n \end{cases} \tag{2}$$

and

$$\tau_{ij}^n = L^n \tau_{ij} \ (j = 1\text{–}3), \ \ \bar{\tau}_{2i}^n = \bar{L}^n \tau_{2i} \quad \text{with } \bar{L}^n = \frac{1}{2h}\int_{-h}^{h}(.)\frac{\mathrm{d}\phi_n}{\mathrm{d}x_2}\mathrm{d}x_2 \tag{3}$$

- weighted form of constitutive equations (n=0–m):

$$\begin{aligned}
\tau_{11}^n &= \alpha\partial_1 u_1^n + \lambda\partial_3 u_3^n + \lambda(S_2^n - \bar{u}_2^n) \\
\tau_{22}^n &= \lambda\partial_1 u_1^n + \lambda\partial_3 u_3^n + \alpha(S_2^n - \bar{u}_2^n) \\
\tau_{33}^n &= \alpha\partial_3 u_3^n + \lambda\partial_1 u_1^n + \lambda(S_2^n - \bar{u}_2^n) \\
\tau_{12}^n &= \mu\partial_1 u_2^n + \mu(S_1^n - \bar{u}_1^n) \\
\tau_{13}^n &= \mu\partial_1 u_3^n + \mu\partial_3 u_1^n \\
\tau_{23}^n &= \mu\partial_3 u_2^n + \mu(S_3^n - \bar{u}_3^n)
\end{aligned} \tag{4}$$

where

$$u_i^n = L^n u_i, \quad \bar{u}_i^n = \bar{L}^n u_i \text{ and } S_i^n = \frac{\hat{S}_i^n \phi_n(1)}{2h} \text{ where } \hat{S}_i^n = \begin{cases} S_i^- = u_i^+ - u_i^- & \text{for even } n \\ S_i^+ = u_i^+ + u_i^- & \text{for odd } n \end{cases} (i = 1\text{–}3) \tag{5}$$

- constitutive equations for face variables:

$$R_i^+ = \mu(\partial_i S_2^+) + \frac{2\mu}{h}\left(\sum_{k=1,3}^{p'} \gamma_k u_i^k + \gamma^- S_i^-\right), \quad R_i^- = \mu(\partial_i S_2^-) + \frac{2\mu}{h}\left(\sum_{k=0,2}^{p} \gamma_k u_i^k + \gamma^+ S_i^+\right) \quad (i = 1,3)$$

$$R_2^+ = \lambda(\partial_1 S_1^+ + \partial_3 S_3^+) + \frac{2\alpha}{h}\left(\sum_{k=1,3}^{p'} \gamma_k u_2^k + \gamma^- S_2^-\right), \tag{6}$$

$$R_2^- = \lambda(\partial_1 S_1^- + \partial_3 S_3^-) + \frac{2\alpha}{h}\left(\sum_{k=0,2}^{p} \gamma_k u_2^k + \gamma^+ S_2^+\right)$$

In Eqs. (1)–(6), $\alpha = 2\mu + \lambda$, where λ and μ are Lamé's constants, ∂_i implies partial differentiation with respect to x_i, and $p = m$ and $p' = m - 1$ for even m and $p = m - 1$ and $p' = m$ for odd m. It is worth mentioning that while deriving Eqs. (1)–(6), it is assumed that ϕ_n is even function of x_2 for even n, and odd function of x_2 for odd n. We may also assume without loss of generality that $\phi_n' = \frac{d\phi_n}{d\bar{x}_2}$ is related to ϕ_j through some coefficients c_{nj} by $\phi_n' = \sum_{j=0}^{m} c_{nj}\phi_j$, implying that $\bar{\tau}_{2i}^n$ and $\bar{u}_i^n$ are related to τ_{2i}^n and u_i^n by

$$(\bar{\tau}_{2i}^n, \bar{u}_i^n) = \frac{1}{h}\sum_{j=0}^{m} c_{nj}(\tau_{2i}^j, u_i^j) \tag{7}$$

The coefficients c_{nj} and the constants γ_j, $\gamma^{\pm}$ appearing in Eqs. (6) and (7) can be determined for any order of theory whenever the distribution functions ϕ_n are chosen. The evaluation of γ_j and $\gamma^{\pm}$ is based on the expansion $u_i = \sum_{k=0}^{m+2} a_k^i \phi_k$, applying to it the operator L^n and the use of constitutive equations (for the details, see Pinarbasi et al., 2006).

3. Application of the approximate theory to elastic layers bonded to extensible reinforcements

Fig. 1a shows the undeformed configuration of an elastic layer of uniform thickness t bonded to flexible reinforcements with equivalent thickness t_f at its top and bottom faces. The deformed configurations of the layer under three simple deformation modes: (i) uniform compression, (ii) pure bending and (iii) pure warping are shown in Fig. 1b–d. In uniform compression mode (Fig. 1b), the layer is compressed uniformly by a uniaxial force P such that the top and bottom reinforcements approach each other with a relative vertical displacement Δ. In pure bending mode (Fig. 1c), the layer is purely bended by bending moments M so that the top and bottom reinforcements *remain plane* and rotate with respect to each other about x_3 axis with a relative angle of rotation ϕ. In pure warping mode (Fig. 1d), the layer is subjected to warping moments Q so that the top and bottom reinforcements deform about x_3 axis with a warping shape $(\pm\Phi/2)\Omega(x_1)$ with *no rotation* from their plane.

The object in this section is to formulate and analyze each problem within the framework of the approximate theory presented in the previous section. In the analyses, the layer is referred to the same rectangular frame employed in the approximate theory. To have the most general form of the governing equations, the reduced form of the relevant equations, in view of the displacement boundary conditions at the top and bottom faces of the layer, are presented by keeping the order of the theory and shape of the cross section arbitrary.

In the derivations and results presented in subsequent sections, the distribution functions in the approximate theory are chosen as Legendre polynomials of the first kind. For this selection, the coefficients c_{nj}, a_k^i, γ_j and $\gamma^{\pm}$ of the theory are as listed in Tables 1 and 2.

Table 1
c_{nj} Coefficients (ϕ_n's are Legendre polynomials)

n	c_{nj} ($j = 0$–m)
0	{0 0 0 0 0}
1	{1 0 0 0 0}
2	{0 3 0 0 0}
3	{1 0 5 0 0}
4	{0 3 0 7 0}

Table 2
Coefficients a_k^i and constants γ_j, $\gamma^{\pm}$ for the 0th, 1st and 2nd order theories (ϕ_n's are Legendre polynomials)

m	a_k^i ($k = 0$–$(m+2)$)	γ_j ($j = 0$–m)	γ^+	γ^-
0	$\{u_i^0 \;\; S_i^-/2 \;\; S_i^+/2 - u_i^0\}$	$\{-3\}$	3/2	1/2
1	$\{u_i^0 \;\; 3u_i^1 \;\; S_i^+/2 - u_i^0 \;\; S_i^-/2 - 3u_i^1\}$	$\{-3 \;\; -15\}$	3/2	3
2	$\{u_i^0 \;\; 3u_i^1 \;\; 5u_i^2 \;\; S_i^-/2 - 3u_i^1 \;\; S_i^+/2 - 5u_i^2 - u_i^0\}$	$\{-10 \;\; -15 \;\; -35\}$	5	3

3.1. Reduced governing equations

Here, the formulations of a flexibly-bonded layer of arbitrary symmetrical section under the three basic deformation modes shown in Fig. 1 are presented within the framework of the approximate theory discussed in Section 2.

3.1.1. Uniform compression

From the deformed configuration shown in Fig. 1b, it is clear that the vertical displacement u_2 is antisymmetric whereas the horizontal displacements u_1 and u_3 are symmetric about the mid-plane of the layer. In other words, the main characteristics of the deformation field for bonded elastic layers remain the same even when the reinforcements are flexible (see Pinarbasi et al., 2006 for the rigid-reinforcement case). Since the distribution functions, are even functions of $\bar{x}_2$ for even n, and odd functions of $\bar{x}_2$ for odd n, one has

$$u_1^n = u_3^n = 0 \;\text{ and }\; \bar{u}_2^n = 0 \text{ for odd } n; \quad \bar{u}_1^n = \bar{u}_3^n = 0 \;\text{ and }\; u_2^n = 0 \text{ for even } n \tag{8}$$

While the flexibility of the reinforcement does *not* affect the form of the "weighted" displacements, it *does* affect the formulation through the "face" displacements, which no longer vanish as they do in the rigid-reinforcement case. Considering that the horizontal displacements are symmetric about the mid-plane of the layer, the face displacements can be written in the following form:

$$u_1^+ = u_1^-, \quad u_3^+ = u_3^- \quad \text{and} \quad u_2^{\pm} = \mp\frac{\Delta}{2} \tag{9}$$

Then, one has

$$S_1^- = S_3^- = S_2^+ = 0, \quad S_1^+ = 2u_1^+ = 2u_1^-, \quad S_3^+ = 2u_3^+ = 2u_3^- \quad \text{and} \quad S_2^- = -\Delta \tag{10}$$

It can be inferred from Eq. (10) that when the reinforcement flexibility is included in the formulation, two additional unknowns appear in the governing equations. Any pair from $\{(S_1^+, S_3^+), (u_1^+, u_3^+), (u_1^-, u_3^-)\}$ can equally be selected as these additional unknowns. In this study, the displacements at the top face of the layer (u_1^+, u_3^+) are used as "unknown face displacements".

Thus, S_i^n can be written in terms of the displacements at the top face of the layer as

$$S_i^n = \begin{cases} 0 & \text{for even } n \\ 2u_i^+/t & \text{for odd } n \end{cases} \text{ for } (i = 1, 3) \quad \text{and} \quad S_2^n = \begin{cases} -\Delta/t & \text{for even } n \\ 0 & \text{for odd } n \end{cases} \tag{11}$$

Then, the constitutive equations for the face variables and the weighted constitutive equations have the following form, in terms of the unknown weighted and face displacements:

- constitutive equations for face variables:

$$R_i^n = \frac{4\mu}{t^2}\left(\sum_{k=0,2}^{p}\gamma_k u_i^k\right) + \frac{8\mu}{t^2}\gamma^+ u_i^+ \quad (i=1,3) \quad \text{for even } n,$$
$$R_2^n = \frac{4\alpha}{t^2}\left(\sum_{k=1,3}^{p'}\gamma_k u_2^k - \gamma^- \Delta\right) + \frac{2\lambda}{t}(\partial_1 u_1^+ + \partial_3 u_3^+) \quad \text{for odd } n \tag{12}$$

- weighted constitutive equations:

$$\left.\begin{aligned}
\tau_{11}^n &= \alpha\partial_1 u_1^n + \lambda\partial_3 u_3^n - \tfrac{\lambda\Delta}{t} - \lambda\bar{u}_2^n \\
\tau_{22}^n &= \lambda\partial_1 u_1^n + \lambda\partial_3 u_3^n - \tfrac{\alpha\Delta}{t} - \alpha\bar{u}_2^n \\
\tau_{33}^n &= \lambda\partial_1 u_1^n + \alpha\partial_3 u_3^n - \tfrac{\lambda\Delta}{t} - \lambda\bar{u}_2^n \\
\tau_{13}^n &= \mu\partial_1 u_3^n + \mu\partial_3 u_1^n
\end{aligned}\right\} \text{ for even } n, \qquad \left.\begin{aligned}
\tau_{12}^n &= \mu\partial_1 u_2^n - \mu\bar{u}_1^n + \tfrac{2\mu}{t}u_1^+ \\
\tau_{23}^n &= \mu\partial_3 u_2^n - \mu\bar{u}_3^n + \tfrac{2\mu}{t}u_3^+
\end{aligned}\right\} \text{ for odd } n \tag{13}$$

and other R_i^n and τ_{ij}^n being zero. Substitution of Eqs. (12) and (13) into Eq. (1) gives the following governing equations for the unknown displacements u_i^n and (u_1^+, u_3^+):

- weighted equilibrium equations:

$$\left.\begin{aligned}
&\left[\alpha\partial_{11}u_1^n + \mu\partial_{33}u_1^n + (\lambda+\mu)\partial_{13}u_3^n - \lambda\partial_1\bar{u}_2^n + \tfrac{4\mu}{t^2}\left(\sum_{k=0,2}^{p}\gamma_k u_1^k\right) + \tfrac{8\mu}{t^2}\gamma^+ u_1^+\right] = \bar{\tau}_{21}^n \\
&\left[\alpha\partial_{33}u_3^n + \mu\partial_{11}u_3^n + (\lambda+\mu)\partial_{13}u_1^n - \lambda\partial_3\bar{u}_2^n + \tfrac{4\mu}{t^2}\left(\sum_{k=0,2}^{p}\gamma_k u_3^k\right) + \tfrac{8\mu}{t^2}\gamma^+ u_3^+\right] = \bar{\tau}_{23}^n
\end{aligned}\right\} \text{ for even } n$$
$$\left[\begin{aligned}
&\mu\partial_{11}u_2^n + \mu\partial_{33}u_2^n - \mu\partial_1\bar{u}_1^n - \mu\partial_3\bar{u}_3^n + \tfrac{4\alpha}{t^2}\left(\sum_{k=1,3}^{p'}\gamma_k u_2^k\right) \\
&\quad - \tfrac{4\alpha}{t^2}\Delta\gamma^- + \tfrac{2(\lambda+\mu)}{t}(\partial_1 u_1^+ + \partial_3 u_3^+)
\end{aligned}\right] = \bar{\tau}_{22}^n \quad \text{for odd } n \tag{14}$$

where $\bar{u}_i^n$ and $\bar{\tau}_{2i}^n$ are related to u_i^n and τ_{2i}^n by, in view of Eq. (7),

$$(\bar{u}_i^n, \bar{\tau}_{2i}^n) = \frac{2}{t}\sum_{j=0}^{m} c_{nj}(u_i^j, \tau_{2i}^j) \tag{15}$$

in which τ_{2i}^j can be expressed in terms of u_i^n and (u_1^+, u_3^+) by Eq. (13).

Due to the appearance of (u_1^+, u_3^+), the number of equations in Eq. (14) is not sufficient to determine all unknowns. Two additional equations for these two additional unknown displacements come from the equilibrium equations written for the reinforcing sheets.

In this study only the monotonically-deformed "interior" bonded layers are considered (Fig. 2). The deformation in a reinforcing sheet is constrained by the deformation of the elastic layers at the top and bottom of the sheet. This constraint is accounted for approximately in the present study through the use of shear stresses at the interfaces between the reinforcing sheet and the layers.

Internal forces on an infinitesimal area of a reinforcing sheet bonded to elastic layers at its top and bottom surfaces are illustrated in Fig. 2, where N_{11} and N_{33} are the stretching forces per unit length in the x_1 and x_3 directions, N_{13} is the in-plane shear force per unit length and τ_{21}^+ and τ_{21}^- are bonding shear stresses. It is assumed that the reinforcing sheet is under the influence of plane state of stress.

Equilibrium equations for the reinforcing sheet in the horizontal directions can be written as, in view of the periodicity conditions in vertical direction for tractions and displacements (these periodicity conditions may be viewed as the reduction of Floquet wave conditions (Brillouin, 1946) for static case),

$$\partial_1 N_{11} + \partial_3 N_{13} = \tau_{21}^+ - \tau_{21}^-, \quad \partial_3 N_{33} + \partial_1 N_{13} = \tau_{23}^+ - \tau_{23}^- \tag{16}$$

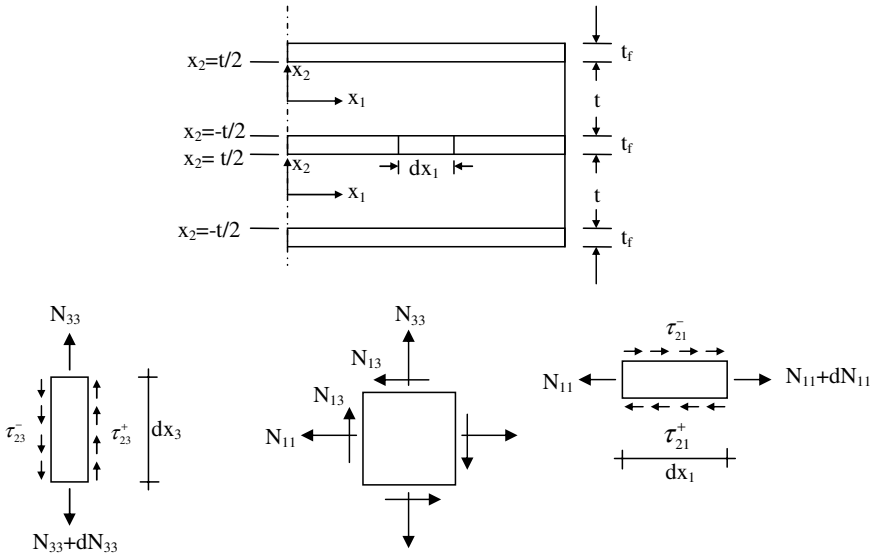

Fig. 2. Forces on an infinitesimal area of a reinforcing sheet bonded to rubber layers at its top and bottom faces (taken from Tsai and Kelly (2001)).

Using the linear elastic stress strain relations, internal forces N_{11}, N_{33} and N_{13} can be expressed in terms of the displacement components as follows:

$$N_{11} = k_f[\partial_1 u_1^+ + v_f \partial_3 u_3^+], \quad N_{33} = k_f[\partial_3 u_3^+ + v_f \partial_1 u_1^+],$$
$$N_{13} = k_f\left(\frac{1-v_f}{2}\right)[\partial_1 u_3^+ + \partial_3 u_1^+] \tag{17}$$

where "in-plane stiffness of the reinforcement" k_f is defined as

$$k_f = \frac{E_f t_f}{1-v_f^2} \tag{18}$$

with E_f and v_f being respectively elasticity modulus and Poisson's ratio of the reinforcing sheet. It should be noted that while writing Eq. (17), perfect bond is assumed between the elastic layer and flexible reinforcements.

Substituting Eqs. (17) and (12), in view of that $R_i^- = \tau_{2i}^+ - \tau_{2i}^- = tR_i^n$ for even n, into Eq. (16), the two additional equations in terms of u_i^n and (u_1^+, u_3^+) can be obtained as

$$\partial_{11} u_1^+ + \frac{1+v_f}{2}\partial_{13} u_3^+ + \frac{1-v_f}{2}\partial_{33} u_1^+ = \frac{1}{k_f}\left[\frac{4\mu}{t}\left(\sum_{k=0,2}^{p} \gamma_k u_1^k\right) + \frac{8\mu}{t}\gamma^+ u_1^+\right]$$
$$\partial_{33} u_3^+ + \frac{1+v_f}{2}\partial_{13} u_1^+ + \frac{1-v_f}{2}\partial_{11} u_3^+ = \frac{1}{k_f}\left[\frac{4\mu}{t}\left(\sum_{k=0,2}^{p} \gamma_k u_3^k\right) + \frac{8\mu}{t}\gamma^+ u_3^+\right] \tag{19}$$

Eqs. (14) and (19) with Eqs. (13) and (15) comprise the reduced governing equations for the compression problem of elastic layers bonded to flexible reinforcements.

3.1.2. Pure bending and pure warping

Bending and warping problems can be treated similarly. Since the reinforcement flexibility does not alter the form of the weighted displacements in Eq. (8), it is sufficient to replace Eq. (9) with

$$u_1^+ = u_1^-, \quad u_3^+ = u_3^- \quad \text{and} \quad u_2^\pm = \begin{cases} \pm\frac{\phi}{2}x_1 & \text{for pure bending} \\ \pm\frac{\phi}{2}\Omega(x_1) & \text{for pure warping} \end{cases} \tag{20}$$

for these problems. Then, one has

$$S_1^- = S_3^- = S_2^+ = 0, \quad S_1^+ = 2u_1^+, \quad S_3^+ = 2u_3^+, \quad \text{and} \quad S_2^- = \begin{cases} \phi x_1 & \text{for pure bending} \\ \Phi\Omega(x_1) & \text{for pure warping} \end{cases} \tag{21}$$

Following the same procedure described for the compression problem, one can obtain the reduced form of the governing equations for the bending and warping problems as

- weighted constitutive equations:

$$\left.\begin{aligned} \tau_{11}^n &= \alpha\partial_1 u_1^n + \lambda\partial_3 u_3^n - \lambda\bar{u}_2^n + \lambda D(x_1) \\ \tau_{22}^n &= \lambda\partial_1 u_1^n + \lambda\partial_3 u_3^n - \alpha\bar{u}_2^n + \alpha D(x_1) \\ \tau_{33}^n &= \lambda\partial_1 u_1^n + \alpha\partial_3 u_3^n - \lambda\bar{u}_2^n + \lambda D(x_1) \\ \tau_{13}^n &= \mu\partial_1 u_3^n + \mu\partial_3 u_1^n \end{aligned}\right\} \quad \text{for even } n$$
$$\tau_{12}^n = \mu\partial_1 u_2^n - \mu\bar{u}_1^n + \tfrac{2\mu}{t}u_1^+, \quad \tau_{23}^n = \mu\partial_3 u_2^n - \mu\bar{u}_3^n + \tfrac{2\mu}{t}u_3^+ \quad \text{for odd } n \tag{22}$$

- weighted equilibrium equations:

$$\left.\begin{aligned} &\left[\alpha\partial_{11}u_1^n + \mu\partial_{33}u_1^n + (\lambda+\mu)\partial_{13}u_3^n - \lambda\partial_1\bar{u}_2^n + \tfrac{4\mu}{t^2}\left(\sum_{k=0,2}^{p}\gamma_k u_1^k\right) + \tfrac{8\mu}{t^2}\gamma^+ u_1^+ \right. \\ &\quad \left. +(\lambda+\mu)\partial_1 D(x_1)\right] = \bar{\tau}_{21}^n \\ &\left[\alpha\partial_{33}u_3^n + \mu\partial_{11}u_3^n + (\lambda+\mu)\partial_{13}u_1^n - \lambda\partial_3\bar{u}_2^n + \tfrac{4\mu}{t^2}\left(\sum_{k=0,2}^{p}\gamma_k u_3^k\right) + \tfrac{8\mu}{t^2}\gamma^+ u_3^+\right] = \bar{\tau}_{23}^n \end{aligned}\right\} \quad \text{for even } n$$
$$\left[\mu\partial_{11}u_2^n + \mu\partial_{33}u_2^n - \mu\partial_1\bar{u}_1^n - \mu\partial_3\bar{u}_3^n + \tfrac{4\alpha}{t^2}\left(\sum_{k=1,3}^{p'}\gamma_k u_2^k\right) + \tfrac{2}{t}(\mu+\lambda)(\partial_1 u_1^+ + \partial_3 u_3^+) + \tfrac{4\alpha}{t}\gamma^- D(x_1)\right] = \bar{\tau}_{22}^n \quad \text{for odd } n \tag{23}$$

- additional equations coming from reinforcement equilibrium:

$$\begin{aligned} \partial_{11}u_1^+ + \frac{1+\nu_f}{2}\partial_{13}u_3^+ + \frac{1-\nu_f}{2}\partial_{33}u_1^+ &= \frac{1}{k_f}\left[\frac{4\mu}{t}\left(\sum_{k=0,2}^{p}\gamma_k u_1^k\right) + \frac{8\mu}{t}\gamma^+ u_1^+ + \mu t\partial_1 D(x_1)\right] \\ \partial_{33}u_3^+ + \frac{1+\nu_f}{2}\partial_{13}u_1^+ + \frac{1-\nu_f}{2}\partial_{11}u_3^+ &= \frac{1}{k_f}\left[\frac{4\mu}{t}\left(\sum_{k=0,2}^{p}\gamma_k u_3^k\right) + \frac{8\mu}{t}\gamma^+ u_3^+\right] \end{aligned} \tag{24}$$

where the "deformation function" $D(x_1)$ is defined as

$$D(x_1) = \begin{cases} \phi x_1/t & \text{for pure bending} \\ \Phi\Omega(x_1)/t & \text{for pure warping} \end{cases}$$

3.1.3. Summary: uniform compression, pure bending and pure warping

It can be recognized that the governing equations for the uniform compression case, i.e., Eqs. (13), (14) and (19), can also be obtained from Eqs. (22)–(24) simply by using $D(x_1) = -\Delta/t$, and so $\partial_1 D(x_1) = 0$. Thus, if the "deformation function" $D(x_1)$ is redefined to include the compression mode as in the following expression:

$$D(x_1) = \begin{cases} -\Delta/t & \text{for uniform compression} \\ \phi x_1/t & \text{for pure bending} \\ \Phi\Omega(x_1)/t & \text{for pure warping} \end{cases} \tag{25}$$

Eqs. (22)–(25), with Eq. (15), comprise the most general form of the reduced governing equations for the analysis of elastic layers bonded to flexible reinforcements under its three basic deformation modes.

3.2. Determination of displacement/stress distributions and effective layer moduli

Eqs. (23)–(25) constitute the three sets of differential equations for the unknown weighted and face displacements $\{u_i^n, u_1^+, u_3^+\}$ governing the behavior of an elastic layer bonded to flexible reinforcements under the three deformation modes shown in Fig. 1. Necessary boundary conditions for the solution of these equations are the traction-free boundary conditions at the lateral bulge-free surfaces of the elastic layer and force-free boundary conditions at the edges of the reinforcing sheets. Once the governing equations are solved for $\{u_i^n, u_1^+, u_3^+\}$, the determination of displacement/stress distributions or any parameter, such as, the effective moduli of the layer, is straightforward.

For various orders of the theory, displacement distributions u_i ($i = 1$–3) may be computed, in terms of u_i^n and $S_i^\pm$, or in terms of $\{u_i^n, u_1^+, u_3^+\}$ in view of Eqs. (10) or (21), from,

$$\begin{aligned} u_i &= u_i^0 + \left(\tfrac{S_i^-}{2}\right)\left(\tfrac{2x_2}{t}\right) + \left(\tfrac{S_i^+}{2} - u_i^0\right)\left(\tfrac{6x_2^2}{t^2} - \tfrac{1}{2}\right) \quad (m=0) \\ u_i &= u_i^0 + (3u_i^1)\left(\tfrac{2x_2}{t}\right) + \left(\tfrac{S_i^+}{2} - u_i^0\right)\left(\tfrac{6x_2^2}{t^2} - \tfrac{1}{2}\right) + \left(\tfrac{S_i^-}{2} - 3u_i^1\right)\left(\tfrac{20x_2^3}{t^3} - \tfrac{3x_2}{t}\right) \quad (m=1) \\ u_i &= \left\{ \begin{array}{l} u_i^0 + (3u_i^1)\left(\tfrac{2x_2}{t}\right) + (5u_i^2)\left(\tfrac{6x_2^2}{t^2} - \tfrac{1}{2}\right) + \left(\tfrac{S_i^-}{2} - 3u_i^1\right)\left(\tfrac{20x_2^3}{t^3} - \tfrac{3x_2}{t}\right) \\ \quad + \left(\tfrac{S_i^+}{2} - u_i^0 - 5u_i^2\right)\left(\tfrac{70x_2^4}{t^4} - \tfrac{15x_2^2}{t^2} + \tfrac{3}{8}\right) \end{array} \right\} \quad (m=2) \end{aligned} \tag{26}$$

Knowing the displacement distributions, the expressions for the stress distributions can be obtained from the stress-displacement relations of linear elasticity.

As discussed in Pinarbasi et al. (2006), effective compression modulus E_c or effective bending modulus E_b of a bonded elastic layer can be obtained from the following relations:

$$E_c = \frac{\sigma_c}{\varepsilon_c} \quad \text{where } \sigma_c = \frac{P}{A} \text{ and } \varepsilon_c = \frac{\Delta}{t} \tag{27}$$

$$E_b = \frac{K_b}{I} \quad \text{and} \quad K_b = \frac{M}{\kappa} \text{ with } \kappa = \frac{\phi}{t} \tag{28}$$

where I is the inertia moment of horizontal layer section about the bending axis. In a similar way, the effective warping modulus E_w can be defined as

$$E_w = \frac{K_w}{J} \quad \text{where } K_w = \frac{Q}{\Phi/t} \text{ and } J = \int_A \Omega^2 \mathrm{d}A \tag{29}$$

where Q is the resultant warping moment and J is the warping inertia (see Tsai and Kelly (2005a,b) for the details). The resultant axial load P in Eq. (27), the resultant bending moment M in Eq. (28) or the resultant warping moment Q in Eq. (29) can easily be obtained, using the following relations, whenever the stress distributions are determined:

$$\begin{aligned} (P, M, Q) &= \iint_A (-\tau_{22}^0, \tau_{22}^0 x_1, \tau_{22}^0 \Omega)\mathrm{d}A \quad \text{for } m = 0 \\ (P, M, Q) &= \iint_A (-\tau_{22}^\pm, \tau_{22}^\pm x_1, \tau_{22}^\pm \Omega)\mathrm{d}A \quad \text{for } m = 1, 2, \ldots \end{aligned} \tag{30}$$

where

$$\tau_{22}^{\pm} = \lambda[\partial_1 u_1^{+} + \partial_3 u_3^{+}] + \frac{2\alpha}{t}\left(\sum_{k=1,3}^{p\prime} \gamma_k u_2^k\right) + 2\alpha\gamma^{-} D(x_1) \tag{31}$$

where $D(x_1)$ is as defined in Eq. (25). Our investigation not reported here indicated that in order to observe the influence of the bonding behavior of elastic layer on bonding stresses $\tau_{2i}^{\pm}$, the order of the theory should be larger than zero. For this reason, τ_{22}^{0}, instead of $\tau_{22}^{\pm}$, is used for $m = 0$ in Eq. (30), which is consistent with the works of Tsai (2004, 2006), where an averaging process is used over the thickness of bonded elastic layer for the evaluation of its effective moduli.

4. Application of the formulation to the infinite-strip-shaped elastic layers bonded to extensible reinforcements

Above three sets of governing equations corresponding to three simple deformation states are derived for a bonded elastic layer of any arbitrary symmetrical shape. In this section, this formulation is applied as illustration to the analysis of "infinitely" long rectangular layers. For each deformation mode, governing equations are solved for displacements, from which closed form expressions for stress distributions and relevant modulus are derived.

In the analysis presented in the following sections, it is assumed that the length of the bonded rectangular layer is much larger than its width $2w$ and thickness t. It is clear that this layer may be approximated by an infinite-strip (IS) shaped bonded layer in a state of plane strain. Thus, for an IS-shaped layer bonded to flexible reinforcements, the displacement along the "infinite" length of the layer vanishes, i.e., $u_3 = 0$, implying that $u_3^{\pm} = 0$. Moreover, the nonzero displacements u_1, u_2 and stretching of the reinforcements in the direction of "finite" length of the layer $u_1^{\pm}$ are independent of x_3, i.e., $u_1 = u_1(x_1, x_2)$, $u_2 = u_2(x_1, x_2)$ and $u_1^{\pm} = u_1^{\pm}(x_1)$.

4.1. Solutions of governing equations

4.1.1. Uniform compression

The compression problem is solved by using both the zeroth order theory (ZOT) and first order theory (FOT). When ZOT ($m = 0$, $p = 0$ and $p' = -1$) is applied to the compression problem, one has, in view of Eqs. (8) and (9), two unknown displacements: one weighted displacement u_1^0 and one face displacement u_1^{+}. The first equation for these unknowns comes from the first of Eq. (14), which in view of Eq. (15) and Tables 1 and 2, can be simplified as

$$\partial_{11} u_1^0 - \beta_{10}^2 [u_1^0 - u_1^{+}] = 0 \quad \text{where } \beta_{10}^2 = \frac{12\mu}{\alpha t^2} \tag{32}$$

The equilibrium of the forces in the reinforcing sheet in x_1 direction generates the second equation for the unknown displacements. Thus, from the first of Eq. (19), in view of Table 2, one has

$$\partial_{11} u_1^{+} - \beta_{11}^2 [u_1^{+} - u_1^0] = 0 \quad \text{where } \beta_{11}^2 = \frac{12\mu}{k_f t} \tag{33}$$

From Eq. (32), it is clear that

$$[u_1^0 - u_1^{+}] = -\frac{1}{\beta_{10}^2}\partial_{11} u_1^0 \tag{34}$$

Substituting Eq. (34) into Eq. (33), one obtains

$$\partial_{11} u_1^{+} = -\frac{\beta_{11}^2}{\beta_{10}^2}\partial_{11} u_1^0 \tag{35}$$

whose solution can be written, in view of that the horizontal displacement u_1 is antisymmetric about $x_1 = 0$, in the form

$$u_1^+ = -\frac{\beta_{11}^2}{\beta_{10}^2}u_1^0 + d_1 x_1 \tag{36}$$

where d_1 is an integration constant to be determined from the boundary conditions. Substitution of Eq. (36) into Eq. (32) gives the following differential equation for the unknown weighted displacement u_1^0:

$$\partial_{11}u_1^0 - \beta_1^2 u_1^0 = -\beta_{10}^2 d_1 x_1 \quad \text{where } \beta_1^2 = \beta_{10}^2 + \beta_{11}^2 \tag{37}$$

When Eq. (37) is solved for u_1^0 and then the solution is substituted into Eq. (36) to determine u_1^+, the following expressions are obtained for the unknown displacements in terms of the two integration constants d_1 and a_{10}:

$$u_1^0 = a_{10}\sinh(\beta_1 x_1) + \frac{\beta_{10}^2}{\beta_{11}^2}d_1 x_1, \quad u_1^+ = -\frac{\beta_{11}^2}{\beta_{10}^2}a_{10}\sinh(\beta_1 x_1) + \frac{\beta_{10}^2}{\beta_{11}^2}d_1 x_1 \tag{38}$$

Noting that the force displacement relations given in Eq. (17) reduce, for the simple strip case, to a single equality: $N_{11} = k_f(\partial_1 u_1^+)$, the constants d_1 and a_{10} can be related by using the force-free boundary condition at the edges of the reinforcement, i.e., by the condition $N_{11}|_{x_1=\pm w} = 0$, as

$$d_1 = a_{10}\frac{\beta_{11}^2\beta_1^3}{\beta_{10}^4}\cosh(\beta_1 w) \tag{39}$$

The second condition for the unknown constants comes from the stress-free boundary conditions at the lateral faces of the layer. While the condition that $\tau_{12}^0|_{x_1=\pm w} = 0$ is satisfied trivially, the condition that $\tau_{11}^0|_{x_1=\pm w} = 0$ implies, in view of the first of Eq. (13) with $n = 0$,

$$[\partial_1 u_1^0]_{x_1=\pm w} = \frac{\lambda \Delta}{\alpha t} \tag{40}$$

which leads to

$$a_{10} = \frac{\lambda}{\alpha}\frac{\Delta}{t}\frac{\beta_{10}^2}{\beta_1^2}\frac{1}{\cosh(\beta_1 w)} \tag{41}$$

Thus, the unknown displacements u_1^0 and u_1^+ can be expressed as

$$u_1^0 = \frac{\lambda}{\alpha}\frac{\Delta}{t}\frac{\beta_{11}^2}{\beta_1^2}\left[x_1 + \frac{\beta_{10}^2}{\beta_{11}^2}\frac{\sinh(\beta_1 x_1)}{\beta_1\cosh(\beta_1 w)}\right], \quad u_1^+ = \frac{\lambda}{\alpha}\frac{\Delta}{t}\frac{\beta_{11}^2}{\beta_1^2}\left[x_1 - \frac{\sinh(\beta_1 x_1)}{\beta_1\cosh(\beta_1 w)}\right] \tag{42}$$

Then, the displacements u_i $(i = 1,2)$ can be computed from the first of Eq. (26) as

$$u_1 = \left\{\begin{array}{l} \frac{3}{2}\frac{\Delta}{t}\frac{\lambda}{\alpha}\frac{\beta_{11}^2}{\beta_1^2}\left[x_1 + \frac{\beta_{10}^2}{\beta_{11}^2}\frac{\sinh(\beta_1 x_1)}{\beta_1\cosh(\beta_1 w)}\right]\left(1 - \frac{4x_2^2}{t^2}\right) \\ \quad + \frac{\Delta}{t}\frac{\lambda}{\alpha}\frac{\beta_{11}^2}{\beta_1^2}\left[x_1 - \frac{\sinh(\beta_1 x_1)}{\beta_1\cosh(\beta_1 w)}\right]\left(\frac{6x_2^2}{t^2} - \frac{1}{2}\right) \end{array}\right\}, \quad u_2 = -\frac{\Delta}{t}x_2 \tag{43}$$

The first of Eq. (43) can be further simplified as

$$u_1 = \frac{3}{2}\frac{\Delta}{t}\frac{\lambda}{\alpha}\frac{\sinh(\beta_1 x_1)}{\beta_1\cosh(\beta_1 w)}\left(1 - \frac{4x_2^2}{t^2}\right) + \frac{\Delta}{t}\frac{\lambda}{\alpha}\frac{\beta_{11}^2}{\beta_1^2}\left(x_1 - \frac{\sinh(\beta_1 x_1)}{\beta_1\cosh(\beta_1 w)}\right) \tag{44}$$

Realizing that the second term on the right hand side of Eq. (44) equals u_1^+ (see the second of Eq. (42)), one, thus, has

$$u_1 = \frac{3}{2}\frac{\Delta}{t}\frac{\lambda}{\alpha}\frac{\sinh(\beta_1 x_1)}{\beta_1\cosh(\beta_1 w)}\left(1 - \frac{4x_2^2}{t^2}\right) + u_1^+ \tag{45}$$

After deriving the displacement distributions, it is not difficult to derive the effective compression modulus for the layer. Using Eq. (27), with the first of Eq. (30), one can obtain the following closed-form expression for the compression modulus E_c:

$$E_c = \alpha - \frac{\lambda^2}{\alpha}\frac{\beta_{10}^2}{\beta_1^2}\frac{\tanh(\beta_1 w)}{(\beta_1 w)} - \frac{\lambda^2}{\alpha}\frac{\beta_{11}^2}{\beta_1^2} \tag{46}$$

It is to be noted that for the rigid-reinforcement case, ZOT leads to the following expressions for the displacements and compression modulus (Pinarbasi et al., 2006):

$$u_1 = \frac{3}{2}\frac{\Delta}{t}\frac{\lambda}{\alpha}\frac{\sinh(\beta_{10}x_1)}{\beta_{10}\cosh(\beta_{10}w)}\left(1 - \frac{4x_2^2}{t^2}\right), \quad u_2 = -\frac{\Delta}{t}x_2, \quad E_c = \alpha - \frac{\lambda^2}{\alpha}\frac{\tanh(\beta_{10}w)}{(\beta_{10}w)} \tag{47}$$

When Eq. (45) and the second of Eq. (43) are compared with the first and second of Eq. (47), it can be concluded that the reinforcement flexibility mainly affects the horizontal displacement of the layer. An additional displacement term appears in u_1 expression. In fact, this term simply equals to the extension of the reinforcement due to the tension generated by the shear stresses developed at the bonded faces of the layer. This additional term is independent of x_2, i.e., it is constant through the layer thickness. It is to be noted that the inclusion of this term in horizontal displacement in flexibly-bonded layers was used as an initial assumption by Kelly (1999) or Tsai (2004); on the other hand, in the present formulation, this is not the assumption, but, the natural consequence of the formulation.

As seen from Eqs. (45) and (47), compared to the rigid-reinforcement case, the inclusion of u_1^+ in the expression of u_1 does not constitute the only modification for the flexible-reinforcement case, but, also the parameter β_{10} is to be replaced by $\beta_1 = \sqrt{\beta_{10}^2 + \beta_{11}^2}$ for the latter case, where β_{11} depends on geometrical and material properties of both the layer (μ, t) and the reinforcing sheets (E_f, v_f, t_f).

As far as the compression modulus E_c is concerned, the expression derived using ZOT is different from that of the pressure method (refer, e.g., to Kelly (2002)). On the other hand, it can be shown that ZOT leads to the same expression derived by Tsai (2004), who eliminated the pressure assumption in his formulation.

Next, the compression problem is analyzed by using FOT. When the order of the theory is one ($m = 1$, $p = 0$ and $p' = 1$), the number of the unknown displacements is three, which are u_1^0, u_1^+ and u_2^1. It is not difficult to show that for $n = 0$, the governing equations of FOT are identical with those of ZOT. Thus, the expressions derived for u_1^0 and u_1^+, i.e., Eq. (42), remain the same in FOT. Using Eq. (15) with Tables 1 and 2 for $m = 1$ and recalling from ZOT that

$$\tau_{22}^0 = \lambda\partial_1 u_1^0 - \frac{\alpha\Delta}{t} \tag{48}$$

the additional variable u_2^1 can be obtained from the solution of nontrivial equilibrium equation in x_2 direction for $n = 1$ (third of Eq. (14)), that is, from

$$\partial_{11}u_2^1 - \frac{60\alpha}{\mu t^2}u_2^1 = \frac{2}{t}\frac{(\lambda+\mu)}{\mu}[\partial_1 u_1^0 - \partial_1 u_1^+] + \frac{10\alpha\Delta}{\mu t^2} \tag{49}$$

From Eq. (42), one has, for the difference $[u_1^0 - u_1^+]$,

$$[u_1^0 - u_1^+] = \frac{\lambda}{\alpha}\frac{\Delta}{t}\frac{\sinh(\beta_1 x_1)}{\beta_1\cosh(\beta_1 w)} \tag{50}$$

which, when inserted into Eq. (49), gives the following equation for u_2^1:

$$\partial_{11}u_2^1 - \beta_{21}^2 u_2^1 = \frac{2}{t}\frac{\lambda+\mu}{\mu}\frac{\lambda}{\alpha}\frac{\Delta}{t}\frac{\cosh(\beta_1 x_1)}{\cosh(\beta_1 w)} + \frac{10\alpha\Delta}{\mu t^2} \quad \text{where } \beta_{21}^2 = \frac{60\alpha}{\mu t^2} \tag{51}$$

Necessary boundary condition for the solution of Eq. (51) comes from the condition that $\tau_{12}^1|_{x_1=\pm w} = 0$, which yields

$$[\partial_1 u_2^1]_{x_1=\pm w} = \frac{2}{t}[u_1^0 - u_1^+]_{x_1=\pm w} \tag{52}$$

which becomes, in view of Eq. (50),

$$[\partial_1 u_2^1]_{x_1=\pm w} = \pm\frac{2}{t}\frac{\lambda}{\alpha}\frac{\Delta}{t}\frac{\tanh(\beta_1 w)}{\beta_1} \tag{53}$$

Since both the differential equation derived for u_2^1 and its boundary conditions in the flexible-reinforcement case are similar to those obtained in the rigid-reinforcement case (see Pinarbasi et al. (2006) for the rigid reinforcement case), the solution derived for the rigid reinforcement case can be adapted to this problem. One can show that the solution derived for u_2 for the rigid-reinforcement case can be used also for the case where the reinforcements are flexible provided that β_1 is used in place of β_{10}.

In view of the above arguments, the displacement distributions and the effective modulus of an IS-shaped layer bonded to flexible reinforcements can be obtained as, under uniform compression,

$$
\begin{aligned}
u_1 &= \frac{3}{2}\frac{\Delta}{t}\frac{\lambda}{\alpha}\frac{\sinh(\beta_1 x_1)}{\beta_1\cosh(\beta_1 w)}\left(1-\frac{4x_2^2}{t^2}\right)+\frac{\Delta}{t}\frac{\lambda}{\alpha}\frac{\beta_{11}^2}{\beta_1^2}\left(x_1-\frac{\sinh(\beta_1 x_1)}{\beta_1\cosh(\beta_1 w)}\right)\\
u_2 &= \left[\frac{30}{t}\frac{\lambda}{\alpha}\frac{\Delta}{t}\frac{x_2}{t}\left(1-\frac{4x_2^2}{t^2}\right).\left\{\begin{array}{l}\frac{1}{\beta_1\beta_{21}}\frac{\tanh(\beta_1 w)}{\sinh(\beta_{21}w)}\left[1-\frac{\mu+\lambda}{\mu}\frac{\beta_1^2}{\beta_1^2-\beta_{21}^2}\right]\cosh(\beta_{21}x_1)\\ +\frac{\mu+\lambda}{\mu}\frac{1}{\beta_1^2-\beta_{21}^2}\frac{\cosh(\beta_1 x_1)}{\cosh(\beta_1 w)}\end{array}\right\}-\frac{\Delta}{t}x_2\right] \qquad (54)\\
E_c &= \alpha-\frac{\lambda^2}{\alpha}\frac{\beta_{10}^2}{\beta_1^2}\frac{\tanh(\beta_1 w)}{(\beta_1 w)}-\frac{\lambda^2}{\alpha}\frac{\beta_{11}^2}{\beta_1^2}
\end{aligned}
$$

When Eq. (54) are compared with Eqs. (43), (44) and (46), it may be seen that increasing the order of the theory from zero to one eliminates the assumption "the plane horizontal section remains plane during deformation", resulting in advanced solutions for the axial displacement distribution and, in turn, for the stress distributions.

4.1.2. Pure bending

This problem is analyzed using only FOT. Recalling that $D(x_1)=\phi\, x_1/t$ for the pure bending case, in the formulation, one has, similar to the compression problem, three unknown displacements, u_1^0, u_2^1 and u_1^+. For these three unknowns, two equations come from the weighted equilibrium equations: the first of Eq. (23) with $n=0$ and the third of Eq. (23) with $n=1$. The third equation is obtained from the equilibrium equation written for the reinforcing sheets: the first of Eq. (24). Two of these equations are independent of u_2^1, as in the compression case. Thus, u_1^0 and u_1^+ can be determined first.

The first of Eqs. (23) with $n=0$ can be reduced, in view of Eq. (15) and Tables 1 and 2 for $m=1$, to the following equation:

$$\partial_{11}u_1^0-\beta_{10}^2\left[u_1^0-u_1^+\right]=-\frac{\lambda+\mu}{\alpha}\frac{\phi}{t}\quad\text{where }\beta_{10}^2=\frac{12\mu}{\alpha t^2} \qquad (55)$$

In a similar way, using the coefficients given in Table 2 for $m=1$, the first of Eq. (24) can be simplified as

$$\partial_{11}u_1^+-\beta_{11}^2\left[u_1^+-u_1^0\right]=\frac{\beta_{11}^2}{\beta_{10}^2}\frac{\mu}{\alpha}\frac{\phi}{t}\quad\text{where }\beta_{11}^2=\frac{12\mu}{k_f t} \qquad (56)$$

Eliminating the terms in the brackets in Eqs. (55) and (56) and then by integrating the resulting equation twice in x_1, the following relation can be obtained between u_1^0 and u_1^+:

$$u_1^+=-\frac{\beta_{11}^2}{\beta_{10}^2}u_1^0-\frac{\beta_{11}^2}{\beta_{10}^2}\frac{\lambda}{\alpha}\frac{\phi}{t}\frac{x_1^2}{2}+d_2 \qquad (57)$$

where d_2 is an integration constant. Unlike the compression problem, in the bending problem, u_1 is symmetric about $x_1=0$. Thus, for u_1^0, one has the following equation:

$$\partial_{11}u_1^0-\beta_1^2u_1^0=\beta_{11}^2\frac{\lambda}{\alpha}\frac{\phi}{t}\frac{x_1^2}{2}-\beta_{10}^2d_2-\frac{\lambda+\mu}{\alpha}\frac{\phi}{t}\quad\text{where }\beta_1^2=\beta_{10}^2+\beta_{11}^2 \qquad (58)$$

from which one can obtain u_1^0 and u_1^+, in view of Eq. (57), as

$$u_1^0 = a_{11}\cosh(\beta_1 x_1) - \frac{\beta_{11}^2}{\beta_1^2}\frac{\lambda}{\alpha}\frac{\phi}{t}\frac{x_1^2}{2} + \frac{1}{\beta_1^2}\frac{\lambda}{\alpha}\frac{\phi}{t}\left[\frac{\beta_{10}^2}{\beta_1^2} + \frac{\mu}{\lambda}\right] + \frac{\beta_{10}^2}{\beta_1^2}d_2$$
$$u_1^+ = -\frac{\beta_{11}^2}{\beta_{10}^2}a_{11}\cosh(\beta_1 x_1) - \frac{\beta_{11}^2}{\beta_1^2}\frac{\lambda}{\alpha}\frac{\phi}{t}\frac{x_1^2}{2} - \frac{\beta_{11}^2}{\beta_{10}^2\beta_1^2}\frac{\lambda}{\alpha}\frac{\phi}{t}\left[\frac{\beta_{10}^2}{\beta_1^2} + \frac{\mu}{\lambda}\right] + \frac{\beta_{10}^2}{\beta_1^2}d_2 \tag{59}$$

where a_{11} is the second integration constant to be determined from the boundary conditions. The condition $N_{11}|_{x_1=\pm w} = 0$, implying $[\partial_1 u_1^+]_{x_1=\pm w} = 0$, leads to

$$a_{11} = -\frac{\beta_{10}^2}{\beta_1^4}\frac{\lambda}{\alpha}\frac{\phi}{t}\frac{\beta_1 w}{\sinh(\beta_1 w)} \tag{60}$$

It should be noted that the nontrivial boundary condition at the lateral bulge-free faces of the layer for $n = 0$, i.e., $\tau_{11}^0|_{x_1=\pm w} = 0$, results in the same expression for a_{11}. The remaining constant d_2 can be obtained from the condition that $[u_1^+]_{x_1=0} = 0$, which yields

$$d_2 = \frac{\beta_{11}^2}{\beta_{10}^4}\frac{\lambda}{\alpha}\frac{\phi}{t}\left[\frac{\beta_{10}^2}{\beta_1^2} + \frac{\mu}{\lambda}\right] - \frac{\beta_{11}^2}{\beta_{10}^2\beta_1^2}\frac{\lambda}{\alpha}\frac{\phi}{t}\frac{\beta_1 w}{\sinh(\beta_1 w)} \tag{61}$$

Then, u_1^0 and u_1^+ become

$$u_1^0 = \left\{-\frac{\beta_{10}^2}{\beta_1^4}\frac{\lambda}{\alpha}\frac{\phi}{t}\frac{\beta_1 w}{\sinh(\beta_1 w)}\left[\frac{\beta_{11}^2}{\beta_{10}^2} + \cosh(\beta_1 x_1)\right] - \frac{\beta_{11}^2}{\beta_1^2}\frac{\lambda}{\alpha}\frac{\phi}{t}\frac{x_1^2}{2} + \frac{1}{\beta_{10}^2}\frac{\mu}{\alpha}\frac{\phi}{t}\left[1 + \frac{\beta_{10}^2}{\beta_1^2}\frac{\lambda}{\mu}\right]\right\}$$
$$u_1^+ = -\frac{\beta_{11}^2}{\beta_1^4}\frac{\lambda}{\alpha}\frac{\phi}{t}\frac{\beta_1 w}{\sinh(\beta_1 w)}[1 - \cosh(\beta_1 x_1)] - \frac{\beta_{11}^2}{\beta_1^2}\frac{\lambda}{\alpha}\frac{\phi}{t}\frac{x_1^2}{2} \tag{62}$$

As already mentioned, the equation for u_2^1 comes from the third of Eq. (23) with $n = 1$, which can be simplified, in view of Eq. (15) and Tables 1 and 2 for $m = 1$, as

$$\partial_{11}u_2^1 - \frac{60\alpha}{\mu t^2}u_2^1 = \frac{2}{t}\frac{(\lambda+\mu)}{\mu}\left[\partial_1 u_1^0 - \partial_1 u_1^+\right] - \frac{10\alpha\phi}{\mu t^2}x_1 \tag{63}$$

From Eqs. (62), it follows that

$$\left[u_1^0 - u_1^+\right] = a_{11}\frac{\beta_1^2}{\beta_{10}^2}\cosh(\beta_1 x_1) + \frac{1}{\beta_{10}^2}\frac{\mu}{\alpha}\frac{\phi}{t}\left[1 + \frac{\beta_{10}^2}{\beta_1^2}\frac{\lambda}{\mu}\right] \tag{64}$$

Using Eq. (64), Eq. (63) can be simplified further to

$$\partial_{11}u_2^1 - \beta_{21}^2 u_2^1 = \frac{2}{t}\frac{\lambda+\mu}{\mu}\frac{\lambda}{\alpha}\frac{\phi}{t}\frac{w\sinh(\beta_1 x_1)}{\sinh(\beta_1 w)} - \frac{10\alpha}{\mu t^2}\phi x_1 \text{ where} \beta_{21}^2 = \frac{60\alpha}{\mu t^2} \tag{65}$$

Necessary boundary condition for the solution of Eq. (65) for u_2^1 is $\tau_{12}^1|_{x_1=\pm w} = 0$, which implies

$$[\partial_1 u_2^1]_{x_1=\pm w} = \frac{2}{t}[u_1^0 - u_1^+]_{x_1=\pm w} \tag{66}$$

which in turn becomes, in view of Eq. (64),

$$[\partial_1 u_2^1]_{x_1=\pm w} = -\frac{2}{t}\frac{\lambda}{\alpha}\frac{\phi}{t}\frac{w}{\beta_1\tanh(\beta_1 w)} + \frac{\phi}{6}\left(1 + \frac{\beta_{10}^2}{\beta_1^2}\frac{\lambda}{\mu}\right) \tag{67}$$

The solution of the governing equation for u_2^1 in the case of flexible reinforcements is almost the same as that derived for the rigid case (see Pinarbasi et al. (2006)) provided that β_{10} is replaced with β_1, which yields

$$u_2^1 = a_{22}\sinh(\beta_{21}x_1) - \frac{2}{t}\frac{\mu+\lambda}{\mu}\frac{\lambda}{\alpha}\frac{\phi}{t}\frac{1}{\beta_1^2 - \beta_{21}^2}\frac{w\sinh(\beta_1 x_1)}{\sinh(\beta_1 w)} + \frac{\phi}{6}x_1 \tag{68}$$

where the constant a_{22} is to be determined from the condition in Eq. (67), which gives

$$a_{22} = \left\{ -\frac{2}{t}\frac{\lambda}{\alpha}\frac{\phi}{t}\frac{w}{\beta_1\beta_{21}}\frac{\coth(\beta_1 w)}{\cosh(\beta_{21}w)}\left[1-\frac{\mu+\lambda}{\mu}\frac{\beta_1^2}{\beta_1^2-\beta_{21}^2}\right] + \frac{\phi}{6}\frac{\lambda}{\mu}\frac{\beta_{10}^2}{\beta_1^2}\frac{1}{\beta_{21}\cosh(\beta_{21}w)} \right\} \tag{69}$$

The displacement components u_i and effective modulus E_b for pure bending case may be obtained from the above expressions of u_1^0, u_1^+ and u_2^1, in view of the second of Eqs. (26) and (28), second of Eqs. (30) and (31). They are

$$\begin{aligned}
u_1 &= \left[-\tfrac{3}{2}\tfrac{\lambda}{\alpha}\tfrac{\phi}{t}\tfrac{w\cosh(\beta_1 x_1)}{\beta_1\sinh(\beta_1 w)} + \tfrac{3}{2}\tfrac{\mu}{\alpha}\tfrac{\phi}{t}\tfrac{1}{\beta_{10}^2}\left(1+\tfrac{\beta_{10}^2}{\beta_1^2}\tfrac{\lambda}{\mu}\right)\right]\left(1-\tfrac{4x_2^2}{t^2}\right) + u_1^+ \\
u_2 &= \left\{ \tfrac{x_2}{t}\left(1-\tfrac{4x_2^2}{t^2}\right).\left(\begin{array}{l} -\tfrac{30}{t}\tfrac{\lambda}{\alpha}\tfrac{\phi}{t}\tfrac{w}{\beta_1\beta_{21}}\tfrac{\coth(\beta_1 w)}{\cosh(\beta_{21}w)}\left[1-\tfrac{\mu+\lambda}{\mu}\tfrac{\beta_1^2}{\beta_1^2-\beta_{21}^2}\right]\sinh(\beta_{21}x_1) \\ \quad +\tfrac{5\phi}{2}\tfrac{\lambda}{\mu}\tfrac{\beta_{10}^2}{\beta_1^2}\tfrac{\sinh(\beta_{21}x_1)}{\beta_{21}\cosh(\beta_{21}w)} - \tfrac{30}{t}\tfrac{\lambda}{\alpha}\tfrac{\phi}{t}\tfrac{\mu+\lambda}{\mu}\tfrac{w}{\beta_1^2-\beta_{21}^2}\tfrac{\sinh(\beta_1 x_1)}{\sinh(\beta_1 w)} \end{array} \right) + \tfrac{\phi}{t}x_1x_2 \right\} \\
E_b &= \left[\begin{array}{l} \alpha - \tfrac{15\lambda\alpha}{\mu}\left\{ \tfrac{\mu+\lambda}{\mu}\tfrac{\beta_{10}^2}{\beta_1^2-\beta_{21}^2}\left[\begin{array}{l} \tfrac{1}{(\beta_1 w)^2}\left(1-\tfrac{\beta_1 w}{\tanh(\beta_1 w)}\right) \\ \quad +\tfrac{1}{(\beta_{21}w)^2}\tfrac{\beta_1 w}{\tanh(\beta_1 w)}\left(1-\tfrac{\tanh(\beta_{21}w)}{\beta_{21}w}\right) \end{array}\right] \right. \\ \left. \quad +\tfrac{1}{(\beta_{21}w)^2}\tfrac{\beta_{10}^2}{\beta_1^2}\left(1-\tfrac{\beta_1 w}{\tanh(\beta_1 w)}\right)\left(1-\tfrac{\tanh(\beta_{21}w)}{\beta_{21}w}\right) \right\} \\ \quad -\tfrac{\lambda^2}{\alpha}\tfrac{\beta_{11}^2}{\beta_1^2}\left\{1+\tfrac{3}{(\beta_1 w)^2}\left(1-\tfrac{\beta_1 w}{\tanh(\beta_1 w)}\right)\right\} \end{array} \right]
\end{aligned} \tag{70}$$

It is worth noting that the prediction of ZOT for E_b has the following simpler form:

$$E_b = \alpha - \frac{3\lambda^2}{\alpha}\frac{\beta_{10}^2}{\beta_1^2}\frac{1}{(\beta_1 w)^2}\left[\frac{(\beta_1 w)}{\tanh(\beta_1 w)}-1\right] - \frac{\lambda^2}{\alpha}\frac{\beta_{11}^2}{\beta_1^2} \tag{71}$$

which reduces to the following equation when $\beta_{11}\to\infty$, or as $\beta_1\to\beta_{10}$,

$$E_b = \alpha - \frac{3\lambda^2}{\alpha}\frac{1}{(\beta_{10}w)^2}\left[\frac{(\beta_{10}w)}{\tanh(\beta_{10}w)}-1\right] \tag{72}$$

which is the prediction of ZOT for E_b of an IS-shaped layer bonded to rigid surfaces.

4.1.3. Pure warping

As already mentioned, the object in this study is to investigate the behavior of bonded elastic layers under three simple deformation modes so that the individual expressions derived for each deformation mode can later be superposed directly to obtain closed-form expressions for the behavior of bonded elastic layers under the combined effects of compression and bending. To simplify the analysis of layers under combined loadings, it is desirable to make compressional, pure bending and warping deformations uncoupled from each other. As the compressional deformation is already uncoupled from pure bending and warping deformations, to achieve this, it is sufficient to choose the warping shape so that the resultant axial force P and bending moment M associated with this warping deformation are zero.

Selecting the simplest cubic function, as proposed by Kelly (1994) and Tsai and Kelly (2005b), is also possible for our study since this assures that the resultant axial force on the layer is zero. In the notation of the present formulation, this expression can be written in the following form:

$$\Omega(x) = \left(\frac{x_1}{w}\right)^3 + f\left(\frac{x_1}{w}\right) \tag{73}$$

The second condition, the condition that the resultant moment on the layer should be zero, then enables one to compute the unknown constant f in Eq. (73). However, it can easily be realized that f cannot be determined at the beginning of the analysis since its computation necessitates knowledge on axial stress distribution, which can be obtained only when the analytical solutions are derived for the displacement components. For this reason, in the following derivations, the constant f is kept as an unknown warping-related parameter until the closed form expressions are obtained for the stress distributions.

In this study, the warping problem, is analyzed using only ZOT, which involves two unknown displacements u_1^0 and u_1^+. Coupled differential equations for u_1^0 and u_1^+ can be obtained from the first of Eq. (23) with $n=0$ and the first of Eq. (24) using the relation given in Eq. (15) and the coefficients and constants given in Tables 1 and 2 for $m=0$, and recalling that $D(x_1)=\Phi\Omega(x_1)/t$ for the warping case. In view of Eq. (73), these equations are

$$\partial_{11}u_1^0-\beta_{10}^2[u_1^0-u_1^+]=-\frac{\lambda+\mu}{\alpha}\frac{\Phi}{t}\left(\frac{3x_1^2}{w^3}+\frac{f}{w}\right)\quad\text{where }\beta_{10}^2=\frac{12\mu}{\alpha t^2} \tag{74}$$

$$\partial_{11}u_1^+-\beta_{11}^2[u_1^+-u_1^0]=\frac{\beta_{11}^2}{\beta_{10}^2}\frac{\mu}{\alpha}\frac{\Phi}{t}\left(\frac{3x_1^2}{w^3}+\frac{f}{w}\right)\quad\text{where }\beta_{11}^2=\frac{12\mu}{k_f t} \tag{75}$$

Eliminating the terms in the brackets in the above equations leads to the following equation:

$$\partial_{11}u_1^+=-\frac{\beta_{11}^2}{\beta_{10}^2}\partial_{11}u_1^0-\frac{\beta_{11}^2}{\beta_{10}^2}\frac{\lambda}{\alpha}\frac{\Phi}{t}\left(\frac{3x_1^2}{w^3}+\frac{f}{w}\right) \tag{76}$$

Keeping in mind that u_1 is an even function of x_1 and integrating Eq. (76) twice in x_1, one has the following relation between u_1^+ and u_1^0:

$$u_1^+=-\frac{\beta_{11}^2}{\beta_{10}^2}u_1^0-\frac{\beta_{11}^2}{\beta_{10}^2}\frac{\lambda}{\alpha}\frac{\Phi}{t}\left(\frac{x_1^4}{4w^3}+f\frac{x_1^2}{2w}\right)+d_2 \tag{77}$$

where d_2 is an integration constant to be determined from boundary and/or symmetry conditions. Substituting Eq. (77) into Eq. (74), the governing equation for u_1^0 is obtained as

$$\partial_{11}u_1^0-\beta_1^2u_1^0=\beta_{11}^2\frac{\lambda}{\alpha}\frac{\Phi}{t}\left(\frac{x_1^4}{4w^3}+f\frac{x_1^2}{2w}\right)-\frac{\lambda+\mu}{\alpha}\frac{\Phi}{t}\left(\frac{3x_1^2}{w^3}+\frac{f}{w}\right)-\beta_{10}^2d_2,\quad\beta_1^2=\beta_{10}^2+\beta_{11}^2 \tag{78}$$

from which one can determine u_1^0 and u_1^+ as, in view of Eq. (77),

$$\begin{aligned}u_1^0&=\left\{\begin{array}{l}a_{11}\cosh(\beta_1x_1)-\frac{\beta_{11}^2}{\beta_1^2}\frac{\Phi}{t}\frac{\lambda}{\alpha}\left[\frac{x_1^4}{4w^3}+\frac{fx_1^2}{2w}\right]\\ \quad+\frac{1}{\beta_1^2}\frac{\lambda}{\alpha}\frac{\Phi}{t}\left[\frac{\mu}{\lambda}+\frac{\beta_{10}^2}{\beta_1^2}\right]\left[\frac{3x_1^2}{w^3}+\frac{f}{w}+\frac{6}{w(\beta_1w)^2}\right]+\frac{\beta_{10}^2}{\beta_1^2}d_2\end{array}\right\}\\ u_1^+&=\left\{\begin{array}{l}-\frac{\beta_{11}^2}{\beta_{10}^2}a_{11}\cosh(\beta_1x_1)-\frac{\beta_{11}^2}{\beta_1^2}\frac{\Phi}{t}\frac{\lambda}{\alpha}\left[\frac{x_1^4}{4w^3}+\frac{fx_1^2}{2w}\right]\\ \quad-\frac{\beta_{11}^2}{\beta_{10}^2\beta_1^2}\frac{\lambda}{\alpha}\frac{\Phi}{t}\left[\frac{\mu}{\lambda}+\frac{\beta_{10}^2}{\beta_1^2}\right]\left[\frac{3x_1^2}{w^3}+\frac{f}{w}+\frac{6}{w(\beta_1w)^2}\right]+\frac{\beta_{10}^2}{\beta_1^2}d_2\end{array}\right\}\end{aligned} \tag{79}$$

where a_{11} is the second integration constant to be evaluated from the boundary/symmetry conditions. Similar to the bending problem, either the force-free boundary conditions at the edges of the reinforcing sheets, $N_{11}|_{x_1=\pm w}=0$, or the stress-free boundary conditions at the lateral surfaces of the layer, $\tau_{11}^0|_{x_1=\pm w}=0$, can be used to determine a_{11}, both of which gives, for a_{11},

$$a_{11}=-\frac{\beta_{10}^2}{\beta_1^2}\frac{\Phi}{t}\frac{\lambda}{\alpha}\frac{1}{\beta_1\sinh(\beta_1w)}\left[1+f+\frac{6}{(\beta_1w)^2}\left(1+\frac{\mu}{\lambda}\frac{\beta_1^2}{\beta_{10}^2}\right)\right] \tag{80}$$

The additional condition for the remaining constant d_2 comes from the condition that $[u_1^+]_{x_1=0}=0$, which results in

$$d_2=a_{11}\frac{\beta_{11}^2\beta_1^2}{\beta_{10}^4}+\frac{\beta_{11}^2}{\beta_{10}^4}\frac{\lambda}{\alpha}\frac{\Phi}{t}\left[\frac{\beta_{10}^2}{\beta_1^2}+\frac{\mu}{\lambda}\right]\left[\frac{f}{w}+\frac{6}{w(\beta_1w)^2}\right] \tag{81}$$

Thus, the weighted displacement u_1^0 and the face displacement u_1^+ become

$$u_1^0 = \left\{ \begin{array}{l} a_{11}\cosh(\beta_1 x_1) + a_{11}\frac{\beta_{11}^2}{\beta_{10}^2} - \frac{\beta_{11}^2}{\beta_1^2}\frac{\lambda}{\alpha}\frac{\Phi}{t}\left[\frac{x_1^4}{4w^3} + \frac{fx_1^2}{2w}\right] + \frac{1}{\beta_1^2}\frac{\mu}{\alpha}\frac{\Phi}{t}\left[1 + \frac{\beta_{10}^2}{\beta_1^2}\frac{\lambda}{\mu}\right]\left[\frac{3x_1^2}{w^3}\right] \\ \quad + \frac{1}{\beta_{10}^2}\frac{\mu}{\alpha}\frac{\Phi}{t}\left[1 + \frac{\beta_{10}^2}{\beta_1^2}\frac{\lambda}{\mu}\right]\left[\frac{f}{w} + \frac{6}{w(\beta_1 w)^2}\right] \end{array} \right\}$$
$$u_1^+ = \left\{ -a_{11}\frac{\beta_{11}^2}{\beta_{10}^2}\cosh(\beta_1 x_1) + a_{11}\frac{\beta_{11}^2}{\beta_{10}^2} - \frac{\beta_{11}^2}{\beta_1^2}\frac{\lambda}{\alpha}\frac{\Phi}{t}\left[\frac{x_1^4}{4w^3} + \frac{fx_1^2}{2w}\right] - \frac{\beta_{11}^2}{\beta_{10}^2\beta_1^2}\frac{\mu}{\alpha}\frac{\Phi}{t}\left[1 + \frac{\beta_{10}^2}{\beta_1^2}\frac{\lambda}{\mu}\right]\left[\frac{3x_1^2}{w^3}\right] \right\} \tag{82}$$

from which the displacement components u_i $(i = 1,2)$ are determined as, in view of the first of Eq. (26),

$$u_1 = \frac{3}{2}\left\{ a_{11}\frac{\beta_1^2}{\beta_{10}^2}\cosh(\beta_1 x_1) + \frac{1}{\beta_{10}^2}\frac{\mu}{\alpha}\frac{\Phi}{t}\left[1 + \frac{\lambda}{\mu}\frac{\beta_{10}^2}{\beta_1^2}\right]\left[\frac{3x_1^2}{w^3} + \frac{f}{w} + \frac{6}{w(\beta_1 w)^2}\right] \right\}\left(1 - \frac{4x_2^2}{t^2}\right) + u_1^+$$
$$u_2 = \frac{\Phi}{t}\left[\frac{x_1^3}{w^3} + f\frac{x_1}{w}\right]x_2 \tag{83}$$

Knowing the expressions for the displacement distributions, expressions for stress distributions can be obtained from linear theory. Then, the constant f appearing in the warping function Ω in Eq. (73) can be determined from the condition that resultant bending moment must be zero in the layer, i.e., from the condition $M = \iint_A (\tau_{22}^0 x_1)\mathrm{d}A = 0$, which yields, for f,

$$f = -\frac{\left\{ \begin{array}{l} \left[1 - \frac{\beta_1 w}{\tanh(\beta_1 w)}\right]\left[1 + \frac{6}{(\beta_1 w)^2}\left(1 + \frac{\mu}{\lambda}\frac{\beta_1^2}{\beta_{10}^2}\right)\right] \\ \quad + 2\left(1 + \frac{\mu}{\lambda}\frac{\beta_1^2}{\beta_{10}^2}\right) - \frac{(\beta_1 w)^2}{5}\frac{\beta_{11}^2}{\beta_{10}^2}\left(1 - \frac{\beta_1^2}{\beta_{11}^2}\frac{\alpha^2}{\lambda^2}\right) \end{array} \right\}}{\left\{ \left[1 - \frac{\beta_1 w}{\tanh(\beta_1 w)}\right] - \frac{(\beta_1 w)^2}{3}\frac{\beta_{11}^2}{\beta_{10}^2}\left(1 - \frac{\beta_1^2}{\beta_{11}^2}\frac{\alpha^2}{\lambda^2}\right) \right\}} \tag{84}$$

Finally, determining Q from the first of Eq. (30) and using the relation defined in Eq. (29), one can compute the warping modulus for an IS-shaped layer bonded to flexible reinforcements as

$$E_w = \frac{\frac{\lambda^2}{\alpha}\frac{\beta_{10}^2}{\beta_1^2}\frac{1}{(\beta_1 w)^2}}{\left(\frac{1}{7} + \frac{2f}{5} + \frac{f^2}{3}\right)}\left\{ \begin{array}{l} \left[\frac{\alpha^2}{\lambda^2}\frac{\beta_1^2}{\beta_{10}^2} - \frac{\beta_{11}^2}{\beta_{10}^2}\right](\beta_1 w)^2\left(\frac{1}{7} + \frac{2f}{5} + \frac{f^2}{3}\right) \\ \quad + \left(1 + \frac{\mu}{\lambda}\frac{\beta_1^2}{\beta_{10}^2}\right)\left(\frac{6}{5} + 2f\right) \\ \quad + \left[\left(1 + f + \frac{6}{(\beta_1 w)^2}\right)\left(1 - \frac{\beta_1 w}{\tanh(\beta_1 w)}\right) + 2\right] \\ \quad \cdot\left[1 + f + \frac{6}{(\beta_1 w)^2}\left(1 + \frac{\mu}{\lambda}\frac{\beta_1^2}{\beta_{10}^2}\right)\right] \end{array} \right\} \tag{85}$$

4.2. Discussions

For a bonded elastic layer, there are two limiting cases with regard to the flexibility of the reinforcing sheets to which the layer is bonded at its top and bottom faces: (i) unbonded and (ii) rigidly-bonded cases. The behavior of a bonded elastic layer approaches to its unbonded behavior when the stiffness of the reinforcing sheets tends to zero and approaches to its rigidly-bonded behavior when their stiffness tends to infinity.

The object in this section is to study the effect of reinforcement flexibility on compressive and bending behavior of bonded elastic layers using the analytical solutions derived in the previous section for IS-shaped elastic layers. To facilitate discussions, the bending behavior of the layers is studied by considering the pure bending and pure warping cases separately. The key parameters chosen in the discussions are: $k_f/\mu t$ (the rigidity of the reinforcing sheets relative to that of the layer), S (shape factor of the layer) and ν (Poisson's ratio of the layer material).

4.2.1. Compressive behavior

Fig. 3a,b show the variation of compression modulus E_c with "stiffness ratio" $k_f^* = k_f/(\mu t)$ for various Poisson's ratios and two specific shape factors; $S = 1$, representing low shape factor (LSF) layers, and $S = 30$, representing high shape factor (HSF) layers. It is to be noted that the shape factor of an IS-shaped layer with a

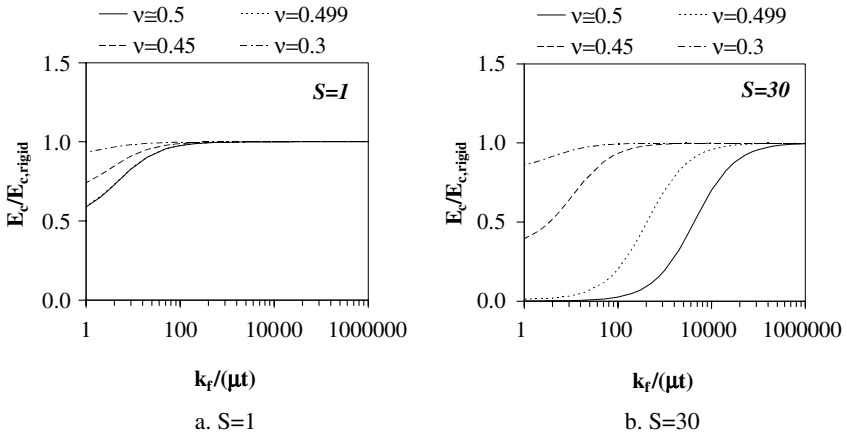

a. S=1 b. S=30

Fig. 3. Effect of reinforcement flexibility on normalized compression modulus of bonded infinite-strip-shaped layers.

thickness t and width $2w$ equals to $S = w/t$. In the plots, E_c values are normalized by the E_c values computed for the equivalent (i.e., with the same S and ν values) rigidly-reinforced layer, denoted as $E_{c,\text{rigid}}$.

As expected, E_c of an elastic layer bonded to flexible reinforcements approaches to $E_{c,\text{rigid}}$ as $k_f^* \to \infty$. While an HSF layer attains its rigid behavior at considerably large values of k_f^*, especially if the layer material is strictly or nearly incompressible, there is no need to have very large values of k_f^* for an LSF layer to behave as if it were rigidly-bonded. Investigation of the behavior of the layers when $k_f^* \cong 30\,000$ is valuable since this value of k_f^*, calculated using $E_f = 210$ GPa, $\nu_f = 0.3$, $t_f = 0.27$ mm, $t = 3$ mm, $\mu = 0.7$ MPa, corresponds to a typical value for the fiber-reinforcement commonly used in seismic isolation bearings (Kelly, 2002; Tsai and Kelly, 2005b). From Fig. 3, it can be seen that the value of 30 000 is a sufficiently large value for the stiffness ratio, even for the HSF layer, to use $E_{c,\text{rigid}}$ instead of E_c in the analysis of layers of nearly incompressible and compressible materials ($\nu \leqslant 0.499$). In Fig. 3b, the curves plotted for $\nu = 0.499$ deviate from the incompressible curves significantly if k_f^* is large. This clearly shows the significance of the inclusion of material compressibility in E_c computations of HSF layers if the reinforcements are inextensible or nearly inextensible.

The graphs presented in Fig. 4 show the effect of reinforcement flexibility on lateral normal stress distributions along the centerline ($x_1 = 0$) in an IS-shaped layer under uniform compression for $S = 1$ and $S = 30$, and for two specific values of k_f^*, 30 000 and 30. The smaller k_f^* value, i.e., 30, is deliberately selected to be so low since, for $S = 1$, reinforcement flexibility becomes effective only when k_f^* is considerably low (Fig. 3a). Similarly, Fig. 5a,b, show shear stress distributions along the vertical section $x_1 = 0.9w$ for $k_f^* = 30$. In the graphs, stress values are normalized with respect to the uniform pressure, i.e., $E_c\varepsilon_c$.

When the graphs in Fig. 4a are compared with similar graphs plotted for the rigid-reinforcement case (see Fig. 3 in Pinarbasi et al. (2006)), it is seen that they are almost identical. This is compatible with the earlier conclusion that the studied layers behave, under compression, as if they were rigidly-bonded when $k_f^* = 30\,000$. From Fig. 4, it can be observed that the lateral normal stress distributions in the LSF layer are not affected significantly from the reinforcement flexibility even when k_f^* is as low as 30. On the other hand, from the graphs plotted for $S = 30$, it is obvious that the effect of k_f^* on the HSF layer is significant: lateral normal stress decreases considerably as k_f^* decreases especially if ν is close to 0.5. It is to be noted that even when $k_f^* = 30$, normal stresses are constant over the layer thickness in the HSF layer.

Fig. 5a,b show that the behavior of the LSF layer is different from that of the HSF layer also with regard to the shear stress distribution: it is linear in the HSF layer, but, can be highly nonlinear in the LSF layer especially if the layer material is compressible.

From the rigid-reinforcement case, it is known that in a bonded elastic layer subject to uniform compression, maximum stresses are experienced at some fixed locations: $(\tau_{22})_{\max}$ at $(x_1 = 0, x_2 = 0)$, $(\tau_{11})_{\max}$ at $(x_1 = 0, x_2 = \pm t/2)$ and $(\tau_{12})_{\max}$ at $(x_1 = \pm w, x_2 = \pm t/2)$. The effect of reinforcement flexibility on these maximum stresses is studied by plotting their variations with k_f^* in Fig. 6a–c for $S = 1$ and 30, and for various values of ν. From Fig. 6a–c, it is observed that while the LSF layer has already reached its incompressible behavior

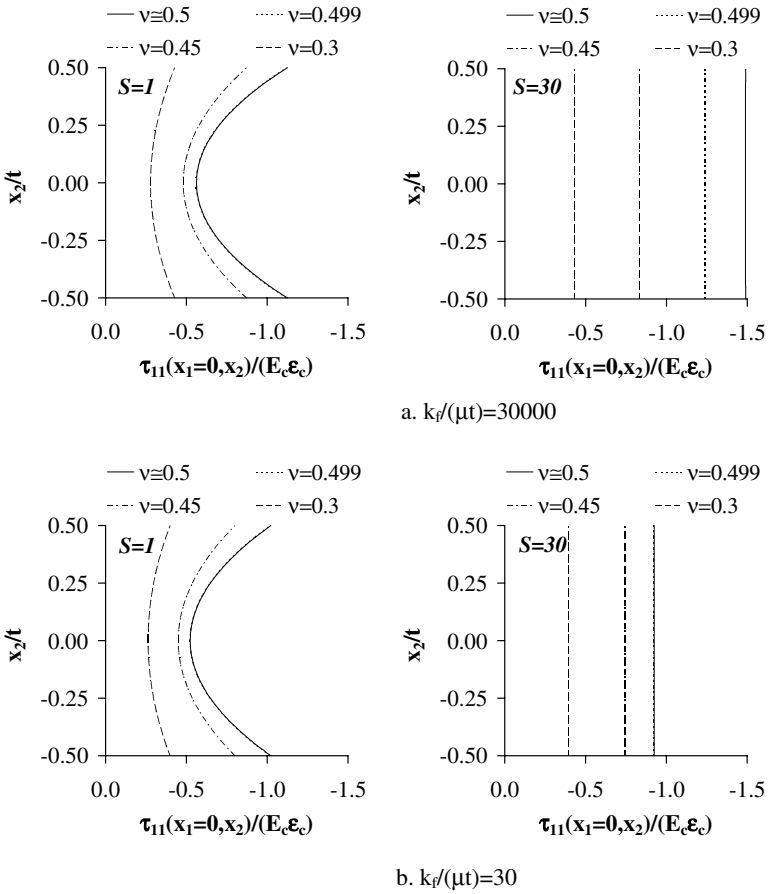

Fig. 4. Effect of reinforcement flexibility on lateral normal stress distribution in axial direction for $S = 1$ and $S = 30$.

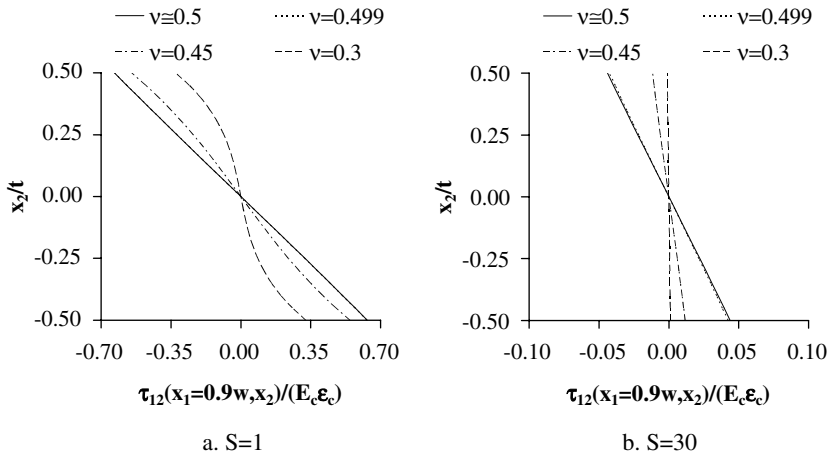

Fig. 5. Effect of reinforcement flexibility on shear stress distribution in axial direction for $k_f/(\mu t) = 30$.

when $v = 0.499$, the behavior of the HSF layer when $v = 0.499$ is considerably different than its incompressible behavior if k_f^* is sufficiently large. From Fig. 6a,b, it may be observed that the main effect of the reinforcement flexibility appears in the decrease of the magnitudes of the maximum normal stresses as k_f^* decreases. Comparison of the graphs in Fig. 6a,b also reveals that the pressure assumption, (i.e., $\tau_{11}=\tau_{22}=\tau_{33}=-p$) is valid

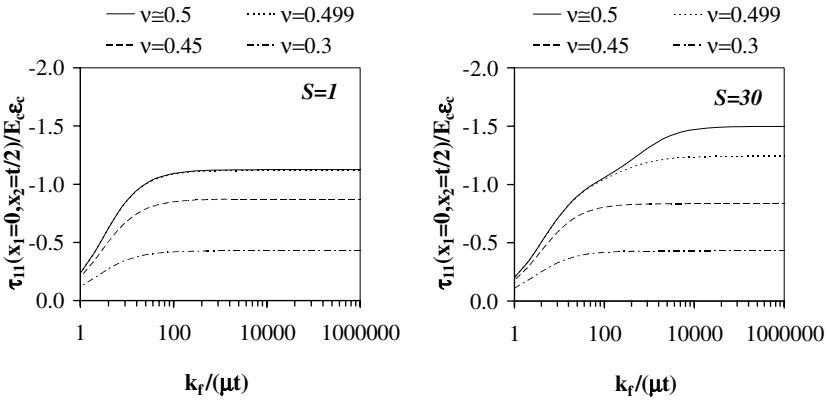

a. maximum lateral normal stress

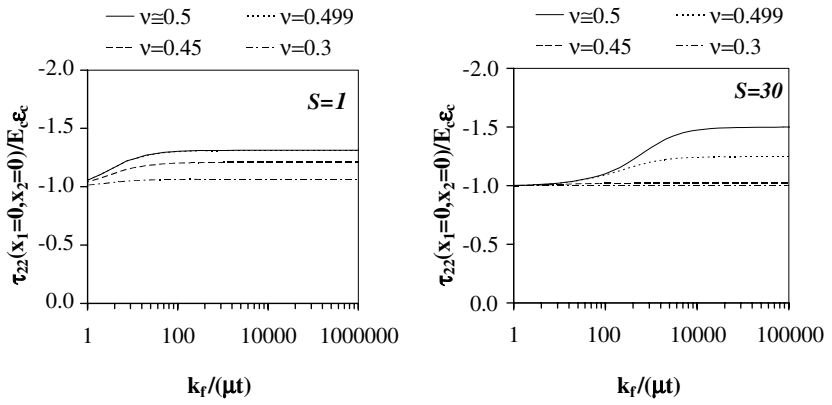

b. maximum axial stress

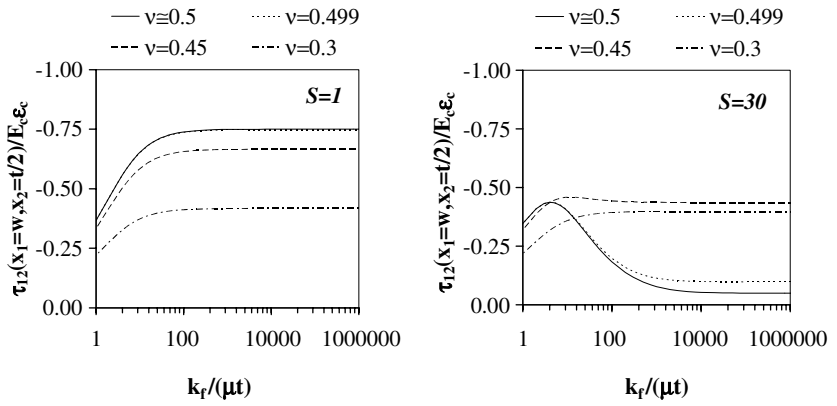

c. maximum shear stress

Fig. 6. Effect of reinforcement flexibility on maximum stresses in a bonded infinite-strip-shaped layer under uniform compression.

only for the HSF layer of nearly/strictly incompressible materials bonded to nearly/strictly inextensible reinforcements.

For the maximum shear stress (Fig. 6c), the reinforcement flexibility affects the LSF and HSF layers differently when $\nu \geqslant 0.499$: as k_f^* decreases, the maximum shear stress decreases in the LSF layer while it increases in the HSF layer until a peak is reached at about $k_f^* = 4$. The bonded elastic layers of compressible materials

($\nu \leqslant 0.45$) start to "sense" the effect of the reinforcement flexibility when k_f^* is considerably low, approximately $k_f^* \leqslant 100$.

4.2.2. Bending behavior

It can be recalled from Section 4.1.2 that ZOT and FOT lead to two different expressions for bending modulus of IS-shaped layers bonded to flexible reinforcements (Eq. (71) and the third of Eqs. (70)). Fig. 7 compares the predictions of ZOT ($m = 0$) and FOT ($m = 1$) for bending modulus E_b for different geometric and material properties, showing that the predictions of both theories match in the studied range of parameters. Considering the complexity of the expression predicted by FOT, it seems to be practical to use the formula of ZOT in the design calculations.

If the graph in Fig. 7a is compared with a similar graph plotted for the rigid-reinforcement case (see Fig. 5 in Pinarbasi et al. (2006)), it is seen that they are almost identical, showing that, as far as the bending modulus is concerned, having a value of 30 000 for the stiffness ratio is sufficient for a bonded IS-shaped layer to behave as if it were rigidly-bonded. The comparison of Fig. 7a with Fig. 7b shows that the reduction of k_f^* from 30 000 to 300 mainly affects HSF layers with low compressibility; E_b values for HSF layers of strictly incompressible

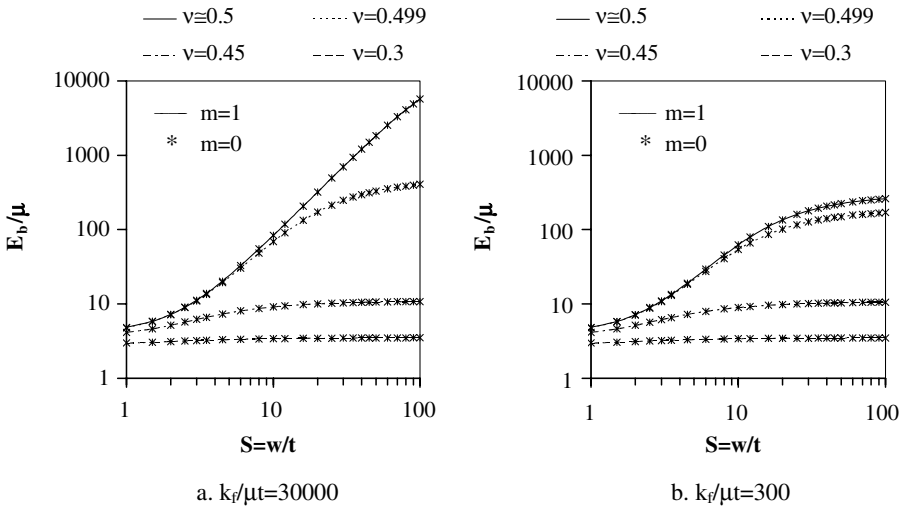

a. $k_f/\mu t=30000$ b. $k_f/\mu t=300$

Fig. 7. Predictions of zeroth and first order theories for bending modulus.

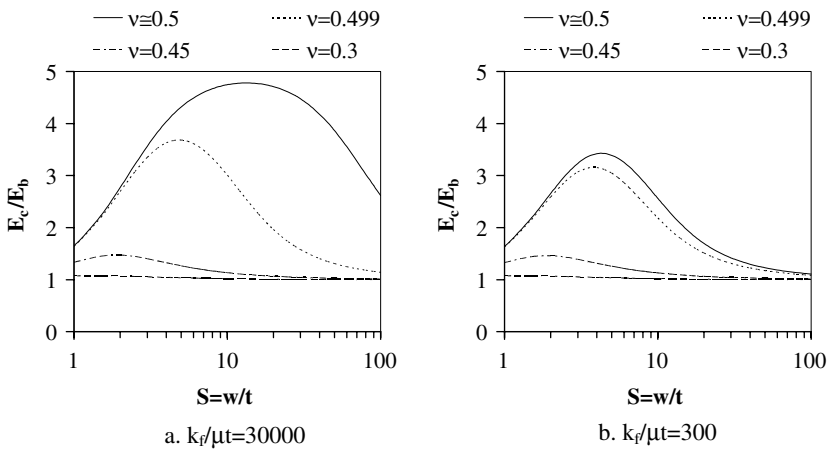

a. $k_f/\mu t=30000$ b. $k_f/\mu t=300$

Fig. 8. Effect of reinforcement flexibility on E_c/E_b ratio.

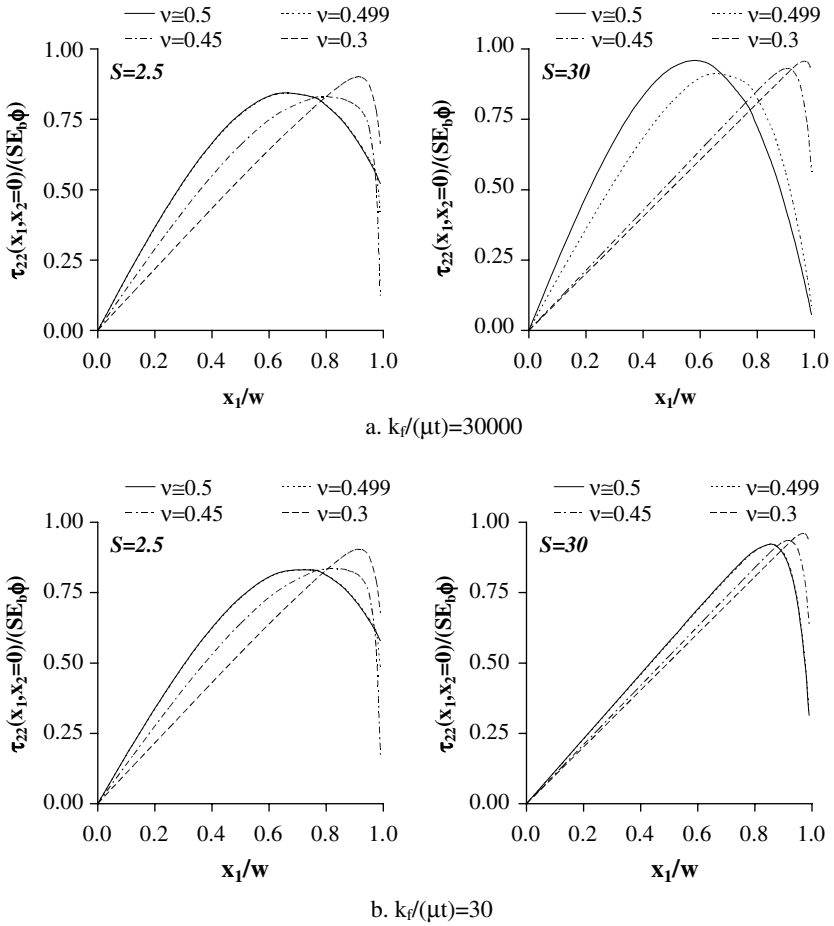

Fig. 9. Effect of reinforcement flexibility on axial stress distribution in lateral direction for $S = 2.5$ and $S = 30$.

materials ($\nu = 0.5$) decrease considerably as k_f^* decreases and approach the E_b values computed for nearly incompressible materials ($\nu = 0.499$).

In design calculations, it is a common practice to represent E_b in terms of E_c. The graphs in Fig. 8 show that the value of E_c/E_b ratio can decrease considerably due to the reinforcement flexibility especially if S and ν are also large. For this reason, taking the value of this ratio as 5, as done in practice, which is suitable only for rigidly-bonded incompressible HSF IS-shaped layers, can significantly underestimate the true value of the bending modulus for layers bonded to extensible reinforcements.

The graphs in Fig. 9 show the effect of the reinforcement flexibility on axial stress distributions in lateral direction in an IS-shaped bonded elastic layer subject to pure bending for various Poisson's ratios, two different shape factors, 2.5 and 30 and two specific values of k_f^*, 30000 and 30. In the graphs, stress distributions are plotted over their most critical sections (i.e., at $x_2 = 0$) and stress values are normalized by $SE_b\phi$.

The graphs in Fig. 9a are close to those plotted for the rigid-reinforcement case with the same S and ν values. Comparison of Fig. 9a and b shows that the bending behavior of the LSF layer is close to its rigidly-reinforced behavior even when $k_f^* = 30$, while the influence of k_f^* on the stress distributions in an HSF layer is significant especially if ν is close to 0.5. From the graphs in Fig. 9 with $S = 30$, it may be observed that the effect of the reinforcement flexibility is very similar to the effect of the material compressibility. As k_f^* decreases, τ_{22} distributions tend to a linear distribution. From Fig. 9b (with $S = 30$), one can also conclude for the bending behavior of HSF layers that the difference between the strictly incompressible and nearly incompressible behaviors is lost as k_f^* decreases. In fact, this conclusion also holds for their compressive behavior (see Fig. 4b with $S = 30$).

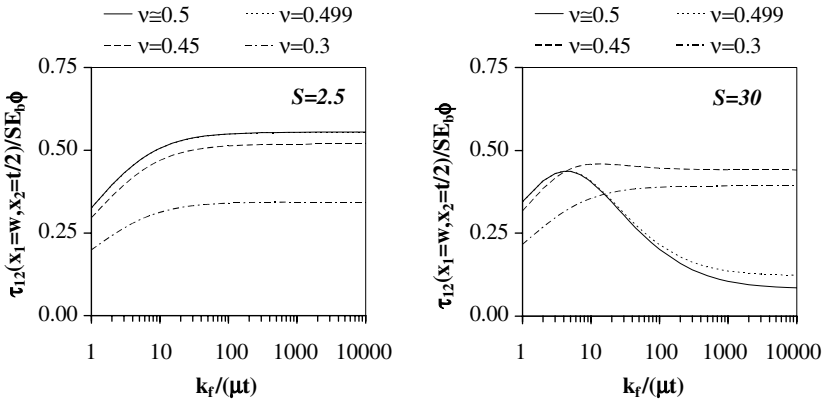

a. S=2.5 b. S=30

Fig. 10. Effect of reinforcement flexibility on maximum normalized shear stress under pure bending.

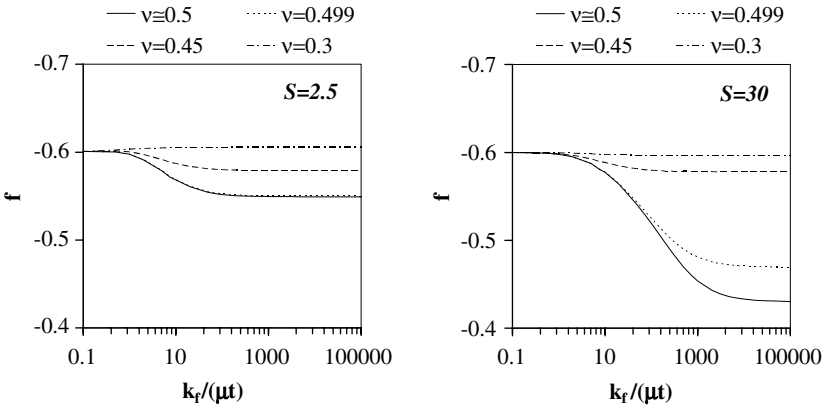

a. S=2.5 b. S=30

Fig. 11. Effect of reinforcement flexibility on warping constant "*f*".

The graphs in Fig. 10 show the effect of reinforcement flexibility on maximum shear stress in an IS-shaped layer under pure bending, which are similar formwise to those of uniform compression case (see Fig. 6c).

4.2.3. Warping behavior

Since the behavior of an elastic layer bonded to extensible reinforcements under pure warping is mainly controlled by the warping pattern of the reinforcements, it is wise to start the discussions in this section with a study of the warping constant "*f*" (Fig. 11).

From Kelly (1994), it can be inferred that there are two limiting values for the warping constant *f*: $f_u = -3/5$, which is the value obtained for an *unbonded* uniform short beam, and $f_b = -3/7$, which is the value predicted by the pressure method for an "incompressible" infinite-strip-shaped layer *bonded* to "inextensible" reinforcements. From Fig. 11, it is seen that *f* approaches f_u as $k_f^* \to 0$, which holds not only for HSF but also for LSF layers. A similar conclusion is *partially* valid for f_b; *f* approaches f_b when $k_f^* \to \infty$ and $v \to 0.5$ only if *S* is sufficiently large since the pressure method is valid only for HSF layers.

To investigate the effect of reinforcement flexibility on the warping modulus E_w thoroughly, its variations with k_f^* are plotted and presented in Fig. 12. In these plots, E_w values are normalized by those calculated using a considerably high value of k_f^*, denoted $E_{w,\text{rigid}}$. When the graphs in Fig. 12 are compared with similar graphs in Fig. 3, it may be observed that k_f^* affects E_w in the same way it affects E_c. However, the effect of the rein-

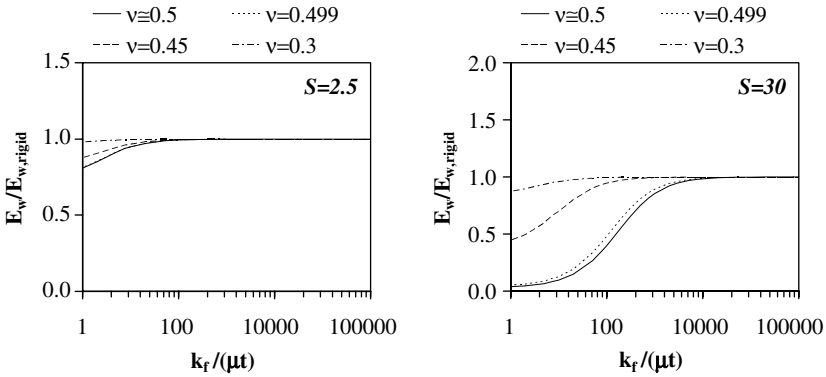

a. S=2.5 b. S=30

Fig. 12. Effect of reinforcement flexibility on normalized warping modulus.

forcement flexibility on E_w is, in general, less than its effect on E_c. For specific values of k_f^*, S and v, the reduction in E_c due to the reinforcement flexibility is larger than that in E_w.

5. Conclusions

This paper presents an extension of the analytical approach proposed by Pinarbasi et al. (2006) for linear analysis of elastic layers bonded to rigid surfaces, to those bonded to flexible reinforcements. Linear behavior of elastic layers bonded to extensible reinforcements with no flexural rigidity under three simple deformation modes, (i) uniform compression, (ii) pure bending and (iii) pure warping, is formulated using an approximate theory based on modified Galerkin method (Mengi, 1980). The proposed formulation improves the displacement and/or stress distributions in bonded elastic layers, compared to the ones considered in literature. The formulations existent in literature (e.g., Kelly, 1999; Tsai, 2004) involve some specific assumptions for displacements and/or stresses in the layer, for example, the assumption of parabolic distribution of bulging displacement over the thickness of the layer, the assumption of the pressure method for stresses, the assumption that plane sections remain plane after the deformation, etc. On the other hand, in the present formulation, the displacement and stress distributions in the layer are represented in terms of a linear combination of a complete set of shape (base) functions, and these distributions are open to improvement by increasing the order of the theory, that is, by increasing the number of the terms (shape functions) considered in the displacement expansions.

In the study, the new formulation is assessed by applying it to the analysis of infinite-strip (IS) shaped elastic layers bonded to extensible reinforcing sheets. Closed form expressions obtained for displacement/stress distributions and three effective moduli, compression, bending and warping moduli, are used to investigate the effects of three key parameters, (i) shape factor S, (ii) Poisson's ratio v and (iii) reinforcement stiffness k_f, on behavior of bonded elastic layers. The following conclusions appear to be valid for the behavior of IS-shaped bonded elastic layers:

- S, v and k_f are the three key parameters that control the behavior of a bonded elastic layer under uniform compression, pure bending or pure warping. They have significant effects not only on the layer stiffnesses but also on the displacement/stress distributions and the magnitude and/or location of the maximum stresses in the layer.
- The behavior of a low shape factor (LSF) layer may be considerably different from that of a high shape factor (HSF) layer. The widely used pressure method seems to be valid only for HSF layers of incompressible or nearly incompressible materials bonded to inextensible or nearly inextensible reinforcements. On the other hand, the stress assumptions of the pressure method, which involve assuming uniform distribution for normal stresses and linear distribution for shear stress over the thickness of the layer, are inconsistent with

the results obtained for LSF layers. Since the normal stress distributions may be highly nonuniform over the layer thickness in an LSF layer, the formulations that "average" the behavior of the layer through the layer thickness can not give accurate solutions for LSF layers while the expressions derived using first order theory can predict the behavior accurately.

- The behavior of a bonded elastic layer approaches asymptotically to its incompressible behavior as Poisson's ratio approaches 0.5. LSF layers reach their incompressible limits at much smaller values of v. For this reason, the behavior of an LSF layer is not influenced significantly from the existence of slight compressibility ($v = 0.499$). On the other hand, the behavior of a slightly compressible HSF layer can be considerably different from its incompressible behavior.
- The behavior of a bonded elastic layer approaches asymptotically to its rigidly-bonded behavior as the reinforcement stiffness tends to infinity. While an HSF layer attains its rigidly-bonded behavior at considerably large values of k_f especially if the layer material is strictly/nearly incompressible, there is no need to have very large values of k_f for an LSF layer to behave as if it were rigidly-bonded.
- In general, the reinforcement flexibility affects the behavior of a bonded elastic layer in the same way the material compressibility does. The behavior of a bonded elastic layer approaches its unbonded behavior as the reinforcement flexibility and/or material compressibility increases. It is important to note that the reinforcement flexibility also changes the effect of the material compressibility: a bonded elastic layer with a smaller k_f reaches its incompressible behavior at a smaller value of v than a layer with the same shape factor, but, with a larger k_f. Similarly, a bonded elastic layer with a smaller v reaches its rigidly-bonded behavior at a smaller k_f value than a layer with the same shape factor, but, with a larger v.
- In design calculations, it is a common practice to represent the bending modulus of a bonded elastic layer in terms of its compression modulus. The commonly used value of 5 for the E_c/E_b ratio is valid only for layers of incompressible materials, high shape factors and rigid reinforcements. It is shown that the use of the above-mentioned value for LSF layers and/or for compressible materials and/or for flexible reinforcements may significantly underestimate the true value of the bending stiffness of the layers.

Acknowledgment

This study is partially funded by the State Planning Organization Grant No: BAP-08-11-DPT2002K120510.

References

Brillouin, L., 1946. Wave propagation in periodic structures. Dover Publications, New York.

Gent, A.N., Lindley, P.B., 1959. The compression of bonded rubber blocks. Proceedings of the Institution of Mechanical Engineers 173 (3), 111–122.

Gent, A.N., Meinecke, E.A., 1970. Compression, bending and shear of bonded rubber blocks. Polymer Engineering and Science 10 (2), 48–53.

Gent, A.N., Henry, R.L., Roxbury, M.L., 1974. Interfacial stresses for bonded rubber blocks in compression and shear. Journal of Applied Mechanics 41, 855–859.

Gent, A.N., 1994. Compression of rubber blocks. Rubber Chemistry and Technology 67 (3), 549–558.

Horton, J.M., Tupholme, G.E., Gover, M.J.C., 2002. Axial loading of bonded rubber blocks. Journal of Applied Mechanics, ASME 69, 836–843.

Kelly, J.M., 1994. The influence of plate flexibility on the buckling load of elastomeric isolators. Report UCB/EERC-94/03, Earthquake Engineering Research Center, University of California, Berkeley, California, USA.

Kelly, J.M., 1997. Earthquake resistant design with rubber. Springer-Verlag, London.

Kelly, J.M., 1999. Analysis of fiber-reinforced elastomeric isolators. Journal of Seismology and Earthquake Engineering 2 (1), 19–34.

Kelly, J.M., Takhirov, S.M., 2001. Analytical and experimental study of fiber-reinforced elastomeric isolators. PEER Report 2001/11, Pacific Earthquake Engineering Research Center, University of California, Berkeley, California, USA.

Kelly, J.M., 2002. Seismic isolation systems for developing countries. Earthquake Spectra 18 (3), 385–406.

Kelly, J.M., Takhirov, S.M., 2002. Analytical and experimental study of fiber-reinforced strip isolators. PEER Report 2002/11, Pacific Earthquake Engineering Research Center, University of California, Berkeley, California, USA.

Lindley, P.B., 1979. Compression moduli for blocks of soft elastic material bonded to rigid end plates. Journal of Strain Analysis 14 (1), 11–16.

Moon, B.-Y., Kong, G.-J., Kong, B.-S., Kelly, J.M., 2002. Design and manufacturing of fiber reinforced elastomeric isolator for seismic isolation. Journal of Materials Processing Technology 130–131, 145–150.

Mengi, Y., 1980. A new approach for developing dynamic theories for structural elements. Part 1: Application to thermoelastic plates. International Journal of Solids and Structures 16, 1155–1168.

Pinarbasi, S., Akyuz, U., Mengi, Y., 2006. A new formulation for the analysis of elastic layers bonded to rigid surfaces. International Journal of Solids and Structures 43, 4271–4296.

Tsai, H.-C., Kelly, J.M., 2001. Stiffness analysis of fiber-reinforced elastomeric isolators. PEER Report 2001/05, Pacific Earthquake Engineering Research Center, University of California, Berkeley, California, USA.

Tsai, H.-C., Kelly, J.M., 2002. Bending stiffness of fiber-reinforced circular seismic isolators. Journal of Engineering Mechanics ASCE 128 (11), 462–470.

Tsai, H.-C., 2004. Compression stiffness of infinite-strip bearings of laminated elastic material interleaving with flexible reinforcements. International Journal of Solids and Structures 41 (24–25), 6647–6660.

Tsai, H.-C., Kelly, J.M., 2005a. Buckling of short beams with warping effect included. International Journal of Solids and Structures 42 (1), 239–253.

Tsai, H.-C., Kelly, J.M., 2005b. Buckling load of seismic isolators affected by flexibility of reinforcement. International Journal of Solids and Structures 42 (1), 255–269.

Tsai, H.-C., 2006. Compression stiffness of circular bearings of laminated elastic material interleaving with flexible reinforcements. International Journal of Solids and Structures 43, 3484–3497.